International Journal of Bifurcation and Chaos, Vol. 18, No. 8 (2008) 2141–2168

METHODS OF THE QUALITATIVE THEORY FOR THE HINDMARSH–ROSE MODEL: A CASE STUDY. A TUTORIAL

ANDREY SHILNIKOV
The Neuroscience Institute and
Department of Mathematics and Statistics,
Georgia State University, Atlanta, USA

MARINA KOLOMIETS
Department of Mathematics,
Academy of Agricultural Sciences,
Nizhniy Novgorod, Russia

Received March 20, 2008; Revised April 3, 2008

Homoclinic bifurcations of both equilibria and periodic orbits are argued to be critical for understanding the dynamics of the Hindmarsh–Rose model in particular, as well as of some square-wave bursting models of neurons of the Hodgkin–Huxley type. They explain very well various transitions between the tonic spiking and bursting oscillations in the model. We present the approach that allows for constructing Poincaré return mapping via the averaging technique. We show that a modified model can exhibit the blue sky bifurcation, as well as, a bistability of the coexisting tonic spiking and bursting activities. A new technique for localizing a slow motion manifold and periodic orbits on it is also presented.

Keywords: Neuron models; tonis spiking; bursting; transition; bifurcation; slow-fast dynamics.

1. Introduction

The Hindmarsh–Rose [Hindmarsh & Rose, 1984] model:

$$\begin{aligned} x' &= y - ax^3 + bx^2 + I - z = P(x, y, \alpha) - z, \\ y' &= c - dx^2 - y = Q(x, y, \alpha), \\ z' &= \varepsilon(s(x - x_0) - z) = \varepsilon R(x, z, \alpha), \end{aligned} \tag{1}$$

remains one of the most popular mathematical models, see [Holden & Fan, 1992; Wang, 1993; Huerta *et al.*, 1997; Izhikevich, 2004; Rosenblum & Pikovsky, 2004; Belykh *et al.*, 2005a; Belykh *et al.*, 2005b; Coombses & Bressloff, 2005] and the references therein, which describes qualitatively well the dynamics of a certain class of neuronal models derived using the Hodgkin–Huxley (HH) formalism [Hodgkin & Huxley, 1952].

A neuron model being a nonlinear system is expected to demonstrate at least three fundamental cell types of activity such as quiescence, tonic spiking and bursting [Coombses & Bressloff, 2006; Kopell, 1988; Rinzel, 1985; Rinzel & Ermentrout, 1989; Wang & Rinzel, 1995; Terman, 1992; Bertram, 1993; Bertram *et al.*, 2000; Izhikevich, 2000]. The nonlinearity of a model may often lead to a bi- or multistability of co-existing cell's activities, which are selected by initial conditions at the same parameter values [Canavier, 1993; Butera, 1998; Cymbalyuk *et al.*, 2002; Bazhenov, 2000; Shilnikov, 2005; Cymbalyuk & Shilnikov, 2005; Shilnikov, 2005; Frohlich & Bazhenov, 2006]. A good neuron model, being a multiparameter family of differential equations, is to describe adequately the transitions between these activities, which are interpreted as the occurrence

of some local and global homoclinic bifurcations [Terman, 1992; Shilnikov, 2005; Guckenheimer, 1993; Kuznetsov & Rinaldi, 1996; Belykh, 2000; Feudel, 2000; Deng, 2002; Shilnikov & Cymbalyuk, 2004; Shilnikov & Cymbalyuk, 2007; Channell *et al.*, 2007a, 2007b]. In the HR model, the x state variable is viewed as the voltage across the cell's membrane, while the "gating" y and z variables describe (in)activations of some current(s). Moreover, the one due to z is a slow current whose rate of change is of order of the small parameter $0 < \varepsilon \ll 1$. Hence the HR model can be called a slow-fast system that has the (x, y)-fast subsystem and the single slow dynamical equation. In this study we set the parameter of the model as follows: $(a = 1, b = 3, c = -3, d = 5, s = 4)$; here $I = 5$, stands for a "synaptic" current. It is easy to see that both I and c are the free terms, and hence all the bifurcations discussed in this paper will be also held for other pairs of I and c. The parameter x_0 is the primary bifurcation one, though we will also consider other values for a, as well as for ε ranging within $[0.002 : 0.02]$, in order to analyze in depth their roles in metamorphoses of the dynamics and conditions for bifurcations in both the model itself and its fast subsystems.

The HR model is known to demonstrate almost all types of robust activities generic for most HH models. It allows also for some regulation of the bursting activity that is often referred to [Rinzel, 1985; Rinzel & Ermentrout, 1989; Terman, 1992] as the square-wave bursting that has been identified in various neuronal models, see [Butera, 1998; Cymbalyuk, 2002; Bazhenov *et al.*, 2000; Chay & Keizer, 1983; Chay, 1985; Bertram & Sherman, 2000; Hill *et al.*, 2001; Gu *et al.*, 2003; Yang *et al.*, 2006], and the references therein. Following the classification proposed in [Bertram, 2000] and enhanced in [Izhikevich, 2000], this type of bursting is also code-named as *fold/homoclinic* indicating that the terminal phases of the slow-fast spiking and slow quiescent periods of a burst are defined through a homoclinic bifurcation of a saddle equilibrium state and a saddle-node bifurcation of equilibria, respectively, which occur in the fast subsystem of the model. It is worth noticing here that the saddle point sets a threshold separating the two co-existing (or transient) states of the neuron, correspondingly: tonic spiking oscillations around the depolarized state, and the hyperpolarized quiescent state. It is their overlapping that creates a hysteresis in the system leading to bursting oscillations, where the solutions of the system switch fast between the above mentioned states, see Fig. 1. One may observe from the waveform that the interspike interval grows by the end of a burst, which is the signature of such square-wave bursters due to the homoclinic bifurcation of the aforementioned saddle. Let us point out that such an increase does not always take place in other square-wave bursters [Shilnikov & Cymbalyuk, 2004, 2005; Shilnikov *et al.*, 2005a, 2005b; Best *et al.*, 2005], where the saddle-node bifurcation of periodic orbits in the fast subsystem is responsible for the terminal phase of bursting.

The classification schemes for differentiating among various kinds of bursting in neuronal models are merely based on distinguishing the mechanisms that initiate or terminate the so-called manifolds of slow motions composed of the limiting orbits, such as equilibria and limit cycles, of the "frozen" fast subsystem in the singular limit $\varepsilon = 0$. Using evident geometric methods based on the slow-fast decomposition, where the slow Z-variable becomes a control parameter, one can detect and follow the branches of equilibria and limit cycles in the fast *planar* subsystem. Note that bifurcations of these limiting sets have been known for almost a century [Andronov & Leontovich, 1937; Andronov *et al.*, 1971], and thus the complete study of such subsystems is quite a trivial problem today. The dynamics of the singularly perturbed system at small $\varepsilon \neq 0$ are known to be determined by and centered around the attracting pieces of these slow motion manifolds [Andronov, 1966; Gradstein, 1946; Tikhonov, 1848; Pontryagin, 1960; Fenichel, 1979; Mischenko & Rozov, 1980; Mischenko *et al.*, 1994; Arnold, 1994]. They constitute a skeleton of the activity patterns in the corresponding slow-fast neuron model. A typical Hodgkin–Huxley model possesses a pair of such manifolds [Rinzel, 1985; Jones Kopell, 1994]: quiescent and tonic spiking, that are denoted by $M_{\rm eq}$ and $M_{\rm lc}$ correspondingly in Fig. 1. The basic problem that limits further development of the theory of slow-fast systems is that the relation between the dynamics displayed by the frozen system and that of the whole slow-fast system is not understood entirely. The slow-fast decomposition allows for the drastic simplification letting one describe clearly the dynamics of a singularly perturbed system. By simply combining the dynamics of both subsystems, one can obtain an adequate description of various dynamical phenomena in the full slow-fast system; this valuable information is scarcely available in all other settings. The drawback of the

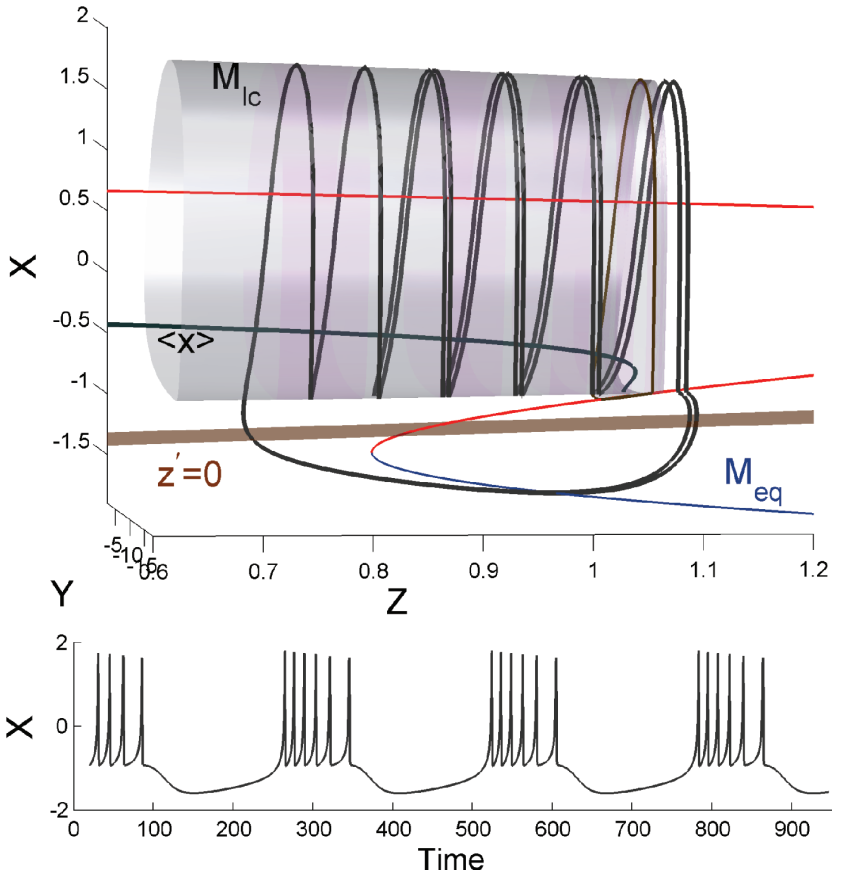

Fig. 1. Square-wave bursting activity in the HR model and the corresponding "voltage" trace for $x_0 = -1.3$, $a = 1$ and $\varepsilon = 0.002$. The spike number within a burst is that of the complete revolutions that the bursting orbit makes around the spiking manifold $M_{\rm lc}$, which is formed of the limit cycles of the fast subsystem (2). Note that the interspike interval grows by the end of a burst: this is a signature of the square-wave bursting, thereby indicating that the phase point approaches the saddle point on the middle section of $M_{\rm eq}$ separating the hyperpolarized (low) and depolarized (upper) states of a neuron.

decomposition approach is evident too, as it does not account for a reciprocal, often complex interactions between the slow and fast dynamics that give rise to potentially new bifurcations occurring in the whole system. It is hardly a surprise that many observed types of dynamics in slow-fast systems cannot be explained within the conventional dissection approach, even though singularly-perturbed systems have been quite a popular study theme for a long time; nevertheless, the number of untouched or incomplete problems remains yet quite large [Guckenheimer, 1996]. For example, the range of new dynamical phenomena present in complex bursting oscillations of many neuron models transcends the existing state of the theory. So, such nonlocal bifurcations, like the blue-sky catastrophe and a few other global bifurcations of saddle and saddle-node periodic orbits [Shilnikov & Cymbalyuk, 2004, 2005; Shilnikov *et al.*, 2005; Channell *et al.*, 2007] in the reduced heart interneuron model, are of codimension-one, i.e. generic and hence can be observed and detected in other models [Doiron *et al.*, 2002; Laing, 2003]. This holds true too for other curious homoclinic bifurcations of the saddle equilibria that generate sudden chaotic explosions in neuronal models [Huerta *et al.*, 2007; Terman, 1992; Deng *et al.*, 2002; Belykh *et al.*, 2002; Feudel *et al.*, 2000; Channell *et al.*, 2007b; Belykh & Shilnikov, 2008; Shilnikov *et al.*, 2008; Malaschenko *et al.*, 2008].

Singular perturbed homoclinic bifurcations of a saddle equilibrium state will be discussed in the HR model, too. We will show that a simple bifurcation of a periodic orbit emerging from a homoclinic loop in the fast subsystem, when singularly-perturbed, becomes degenerate and transforms into the homoclinic orbit-flip bifurcations [Shilnikov, 1998, 2001]. We will argue that the transition between tonic spiking and bursting in the model can be fully understood within the framework of the theory of

homoclinic bifurcations of codimension-2 that turns out to be a generic property of such slow-fast systems. One of the features of the orbit-flip bifurcation is that its unfolding includes a quick cascade of period-doubling bifurcations of periodic orbits. Recall that a sequence of such bifurcations leads to or precedes the frequently observed phenomenon of chaotization of dynamics at the transition from tonic spiking to bursting in various square-wave bursters [Terman, 1992; Shilnikov *et al.*, 2005; Cymbalyuk & Shilnikov, 2005; Rowat & Elson, 2004].

In the final part of this paper we will discuss some geometrical rearrangements and conditions under which the HR model may exhibit two distinct homoclinic bifurcations of the saddle-node periodic orbit. One of them is the *blue-sky catastrophe* [Turaev & Shilnikov, 1999; Shilnikov & Turaev, 1997]. This striking term [Abraham, 1985] is given to the last, of the seven known, primary (i.e. codimension one) stability boundaries of periodic orbits. While the first six boundaries had been known for 70 years [Andronov & Leontovich, 1937; Andronov *et al.*, 1971], the blue-sky catastrophe was discovered and analyzed only recently [Shilnikov & Turaev, 2000; Gavrilov & Shilnikov, 2000; Shilnikov *et al.*, 2004; Shilnikov *et al.*, 2001]. This bifurcation turns out to be a typical phenomenon for multiple-scale systems [Shilnikov *et al.*, 2001; Shilnikov *et al.*, 2005]. Of special, fundamental interest is its perspective for computational neuroscience where the blue-sky catastrophe describes a continuous and reversible transition between periodic bursting and tonic spiking in the reduced heart interneuron model [Shilnikov & Cymbalyuk, 2004, 2005].

The dynamical feature of the second bifurcation is the bistability of co-existing tonic spiking and bursting in the system [Shilnikov *et al.*, 2005; Cymbalyuk *et al.*, 2005]. The organizing center for this configuration is another saddle-node bifurcation, first introduced by Lukyanov and Shilnikov [1978], which describes the disappearance of a saddle-node periodic orbit with the so-called noncentral homoclinics. Moreover, near this bifurcation the HR model is shown to fire an unpredictable, chaotic number of burst trains before it settles down into the periodic tonic spiking attractor. This intermittency is a consequence of Smale-horseshoe shift dynamics in the model [Channell *et al.*, 2007a, 2007b; Gavrilov & Shilnikov, 1973].

The rigorous results based on the methods of the qualitative theory [Shilnikov *et al.*, 1998, 2001] and implemented numerically [Kuznetsov, 1998] for the Hindmarsh–Rose model are not limited to it solely but can be employed effectively in studies of various models of cortical neurons and those forming central pattern generators.

2. 2D Hindmarsh–Rose Model

The limit $\varepsilon = 0$ singles out the fast subsystem

$$\begin{aligned} x' &= y - ax^3 + 3x^2 + 5 - z = P(x, y, \alpha) - z, \\ y' &= -3 - 5x^2 - y = Q(x, y, \alpha), \end{aligned} \tag{2}$$

of the Hindmarsh–Rose model, where the frozen z-variable is now the bifurcation parameter. We will begin analyzing its equilibria and their bifurcations as z is varied. The numerical section of the analysis is performed using the software package Content [Kuznetsov, 1998].

An equilibrium state of (2) lies in the (x, y)-phase plane at the intersection of two nullclines given by $P(x, y, \alpha) - z = 0$ and $Q(x, y, \alpha) = 0$. Variations of z make the graph of the former move in the phase plane; so does synchronously the equilibrium state. The right-hand side of the fast subsystem was tailored specifically by the authors of the model so that it would have typically one or three equilibrium states. The coordinate dependence of the equilibrium states of (2) on z is summarized in Fig. 2. In the *extended* (z, x, y)-phase space, the space curve labeled $M_{\rm eq}$ is composed of all equilibrium states of (2). Its stable and unstable segments (read equilibria) are shown in blue and red, respectively. The primary feature of $M_{\rm eq}$ is its Z-shape, where the upper and lower branches are associated with the de- and hyper-polarized states of the modeled neuron.

One can see from the bifurcation diagram in Fig. 2 that when the parameter z is small, the fast subsystem has a single stable equilibrium state corresponding to a depolarized state of the neuron. As z is increased, this equilibrium state becomes unstable through a super-critical Andronov–Hopf bifurcation. The type of bifurcation and the stability of the bifurcating equilibrium state are determined by the sign of a first Lyapunov coefficient that turns out to be *negative* in this case. This means that a single, stable limit cycle emerges from the equilibrium state as the Z-parameter is increased. By varying z, we can continue the paraboloid-shaped branch $M_{\rm lc}$ composed of the limit cycles of the fast subsystem. The space curves labeled as $x_{\max}$ and $x_{\min}$ in Fig. 2 help us figure out the way the size

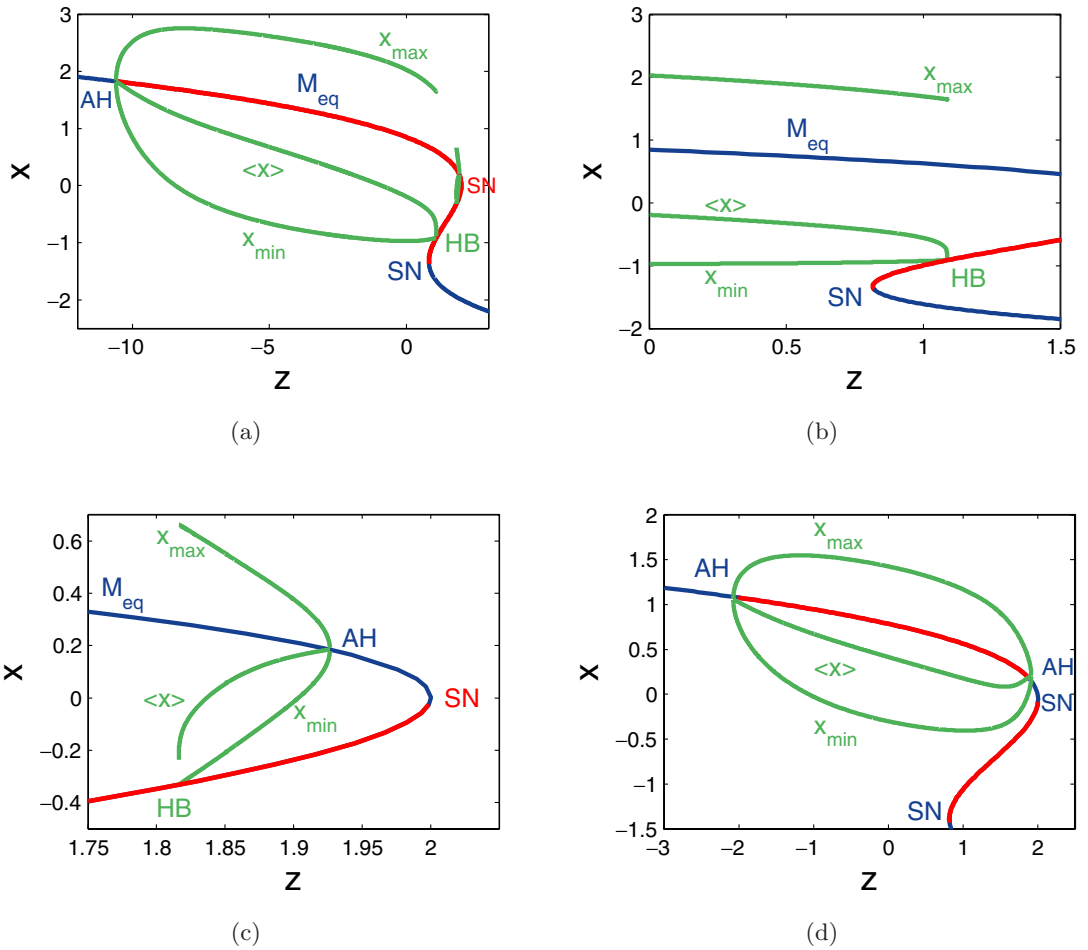

Fig. 2. Bifurcation diagrams showing the dependence of the x-coordinates of the equilibrium states and the limit cycles of the fast subsystem (2) on the control parameter z for $a = 1$ in (a)–(c), and for $a = 1.6$ in (d). Shown in red and blue are the segments composed of unstable and stable equilibria of (2). Here, the branches $x_{\min}$, $x_{\max}$ and $\langle x\rangle$ stand respectively for the minimal, maximal and average values of the coordinates of the limit cycles. Note that in insets (a)–(c) the limit cycle branch terminates through the homoclinic bifurcations of a saddle in the middle section of $M_{\rm eq}$. In contrast, in inset (d) this branch both emerges and ends through the supercritical Andronov–Hopf bifurcations because the z-parameter pathway no longer gets through a homoclinic bifurcation when $a = 1.6$, as shown in Fig. 4.

of the limit cycle changes. This is the core of the parameter continuation technique that is so obvious in the planar case. We will enhance this approach below to locate similar, though less trivial, manifolds in the whole model. The branch labeled by $\langle x\rangle$ in the figure shows the dependence of the coordinates of a "gravity center" of the limit cycle, i.e. its coordinates averaged over its period:

$$\langle \mathbf{x}(z)\rangle = \frac{1}{T(z)}\int_0^{T(z)} \phi(t;z)\,dt; \tag{3}$$

here $\mathbf{x} = \phi(t;z)$ ($\mathbf{x} = (x,y)$) is meant to be the equation of the limit cycle of period $T(z)$ in the fast subsystem. Observe from Fig. 2 that as z increases, the branch $\langle x\rangle$ approaches $x_{\min}$.

Before both branches merge, another equilibrium states of (2) emerge from a saddle-node bifurcation. This occurs with the tangency of the aforementioned nullclines that produces a double equilibrium state that further splits into a node, O_h and a saddle, O_s. This bifurcation takes place on the fold or the lower turning point of the manifold $M_{\rm eq}$. The phase plane of the fast subsystem (2) with its three equilibrium states is depicted in Fig. 3.

To determine the stability of the node, one needs to evaluate the trace $P_x + Q_y$ of the Jacobian $\begin{vmatrix} P_x & P_y \\ Q_x & Q_y \end{vmatrix}$ of (2) at the bifurcation point. If it is negative, which is so in our case, then the node will be stable. Continuation of the stable node and saddle branches completes the Z-shaped branch $M_{\rm eq}$ of the

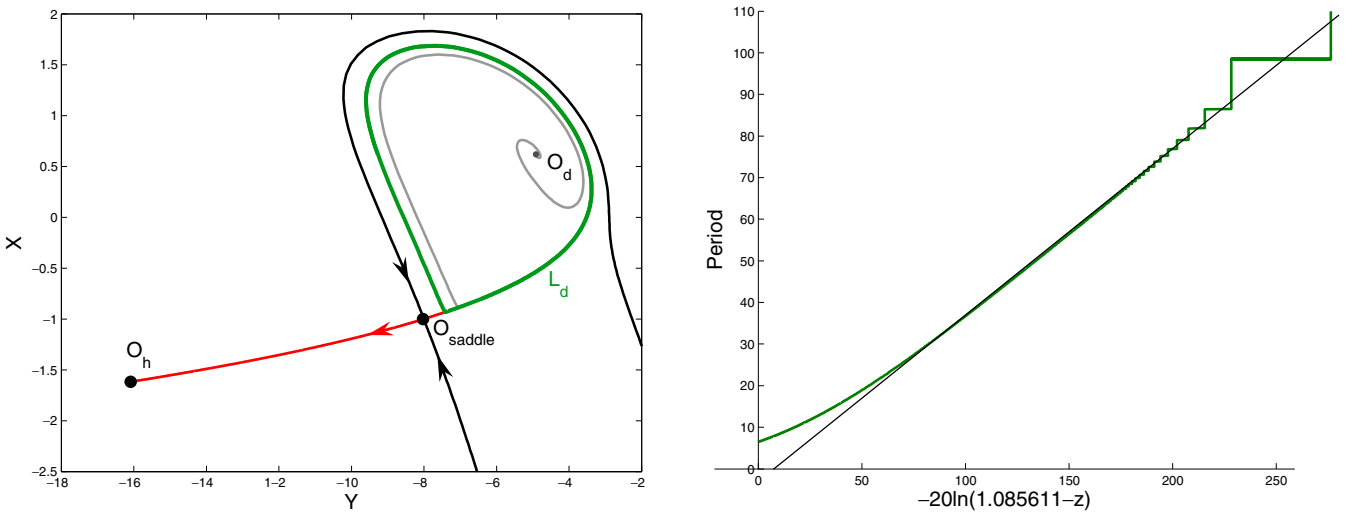

Fig. 3. (Left) Phase portrait of the fast subsystem (2) at $z = 1$. The stable separatrix of the saddle O_s divides the phase plane into the attraction basins of the stable limit cycle L_d and the stable hyperpolarized state O_h. For $a = 1$, as z is increased further, the limit cycle approaches the saddle becoming its homoclinic loop. (Right) The period of the limit cycle grows logarithmically fast towards the homoclinic bifurcation at $z \simeq 1.0856$.

equilibrium states of the fast subsystem. The lower branch of $M_{\rm eq}$, which is thus composed of the stable equilibrium states, is associated with a hyperpolarized state of a neuron.

Both de- and hyperpolarized branches of $M_{\rm eq}$ are bridged by the *threshold* segment consisting of the saddles of the fast subsystem (2). The sign of the so-called *saddle value* σ of each saddle equilibrium state is determined by that of the trace of the above Jacobian in a planar case. By construction, this saddle value σ is the sum of the positive and negative characteristic exponents of the saddle. These exponents determine the unstable and stable directions that are tangent to the one-dimensional stable and unstable separatrices of the saddle, see Fig. 3. One can observe from this figure that the stable (incoming) separatrix breaks the (x, y)-phase plane into the attraction basins of the stable limit cycle and the stable hyperpolarized node O_h.

The stable and unstable separatrices coincide at some $z_h \simeq 1.0856$ thereby forming a homoclinic loop of the saddle. This configuration corresponds to a simple codimension-one homoclinic bifurcation in the system. It was shown in [Andronov & Leontovich, 1937] that this bifurcation generates a single, simple limit cycle in the phase plane if the saddle value $\sigma \neq 0$. The sign of σ determines the stability of the limit cycle: it is born stable when $\sigma < 0$ and unstable otherwise. The other fact worth noticing from the homoclinic bifurcation theory is that the period of the limit cycle grows logarithmically fast, i.e. as $-\ln|z_h - z|$, as it approaches the saddle, see Fig. 3. This explains the increase of the interspike intervals by the end of bursts in Fig. 1. Moreover, since the size of the limit cycle remains finite, the average branch $\langle x \rangle$ of the limit cycles adjoins to the saddle segment of $M_{\rm eq}$ with a vertical tangent.

Let us point out that the choice of the factors of the polynomial terms in the right-hand side of (2) is quite accurate. This means that should the factors be slightly different, one can easily miss the homoclinic bifurcation on the z-parameter pathway at other, larger values of the parameter a. This point is illustrated in Fig. 2(d), where the limit cycles branch $M_{\rm lc}$ both begins and ends through the forward and reverse supercritical Andronov–Hopf bifurcations. Actually, both bifurcations occur on the same bifurcation curve in the (z, a)-parameter plane of the fast subsystem (2), which gets through the z-passway twice. One sees clearly that in contrast to the "homoclinic" case at $a = 1$, the elevation of a to 1.6 implies that the corresponding z-pathway no longer crosses the homoclinic bifurcation curve in the bifurcation diagram shown in Fig. 4(a). We will return to the consequences of this fact below where we will consider transitions from square-wave to plateau-shaped bursters in the HR model (Fig. 8). Meanwhile, one may wonder about the secondary branch $M^2_{\rm lc}$ that originates from the reverse AH bifurcation. As inset (c) in Fig. 2 reveals out that there is a secondary homoclinic bifurcation at $z \simeq 1.82$ on the z-pathway at $a = 1$. Interestingly,

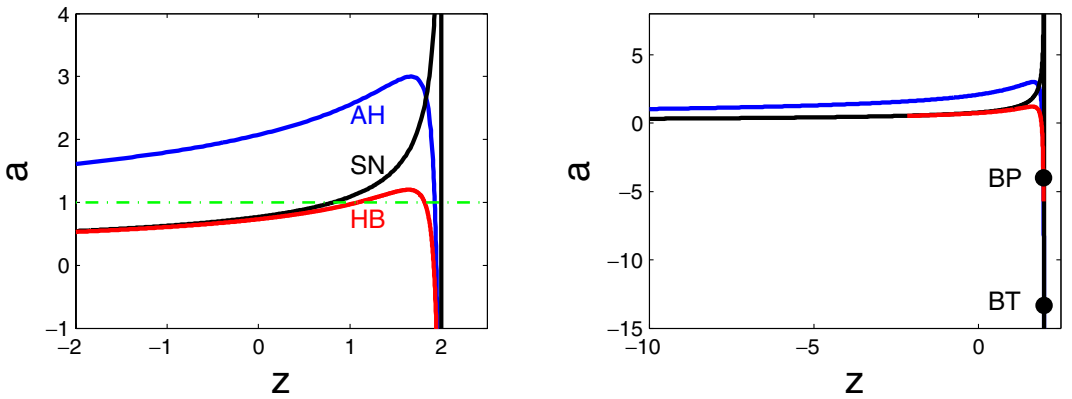

(a) (b)

Fig. 4. The (z, a)-parameter plane of the fast subsystem (2). The labels AH, SN and HB stand for the Andronov–Hopf, saddle-node and homoclinic bifurcations. The Bautin point, BP, breaks the AH-curve into super- and sub-critical branches. The AH curve originates from this cod-2 point, where the system has an equilibrium state with double zero characteristic exponents, the so-called Bogdanov–Takens (BT) bifurcation. The z-pathway at $a = 1$ goes across all three bifurcation curves. However, making a greater than 1.213281 elevates the pathway so that no homoclinic bifurcation occurs on it. This means that the cycle must undergo a reverse Andronov–Hopf bifurcation where it collapses back into the depolarized focus O_d as z is increased, see Fig. 2(d).

this may lead to bursting oscillations of peculiar shapes in the HR model, when the phase point drifts along the saddle branch and then switches by either dropping down onto hyperpolarized branch of $M_{\rm eq}$ or raising up to the secondary spiking branch of $M^2_{\rm lc}$.

3. Bifurcations in the Hindmarsh–Rose Model

When ε is no longer zero, then z is no longer the frozen but a slow dynamical variable. Since the last equation of the HR model (1) is linear in both x and z, the rate of change of z is of the order of ε. Moreover, this linearity helps one understand better our analysis of the model, though one should not rely on this property. In our simulations we will keep ε reasonably small.

As the slow equation contains no y-variable, the plane in the (z, y, x)-phase space of the HR model where the time derivative z' vanishes is called a *slow nullcline*. One can see that $z' < 0$ and $z' > 0$ below and above this nullcline. By varying the bifurcation parameter x_0 we lower and elevate the nullcline in the phase space.

3.1. *Equilibrium states*

The coordinates of the equilibrium state of the HR model do not depend on ε but its stability does. Therefore, in the phase space of the HR model, which is the extended phase space of its fast subsystem, the equilibrium state is the point where the slow nullcline $z' = 0$ crosses the earlier introduced 1D space branch $M_{\rm eq}$ composed of the equilibrium states of the fast subsystem. Hence, by varying the parameter x_0, we shift the slow nullcline thereby shifting the intersection point thus making the equilibrium state slide along $M_{\rm eq}$, see Fig. 5. Therefore, in order to localize the desired branch $M_{\rm eq}$ in the phase space we can skip the slow-fast dissecting and instead directly trace $M_{\rm eq}$ down as the x_0-*parametric* branch composed of the equilibrium states of the full system. This simple observation leads to a very effective way for finding such slow manifolds in high-dimensional neuron models with several time scales where the proper dissection is often problematic. Basically, all one needs is to figure out the slowest equation(s), and choose a "scanning" parameter in it to vary without reshaping the nullclines. Furthermore, such a parameter can be even introduced artificially for a similar purpose too, like an external injected current. The interpretation of bifurcations of equilibria on $M_{\rm eq}$ is another issue.

Let us give the interpretation and find out a way the bifurcations on $M_{\rm eq}$ in the fast and full systems relate.

We will follow the x_0-parametric pathway illustrated in Fig. 5, where x_0 decreases from 5 through -2. Let the slow nullcline $z' = 0$ first get through $M_{\rm eq}$ to the left of the AH point on $M_{\rm eq}$. Here, the equilibrium state is stable in the (y, x)-space, as well as in z, because in restriction to the slow manifold

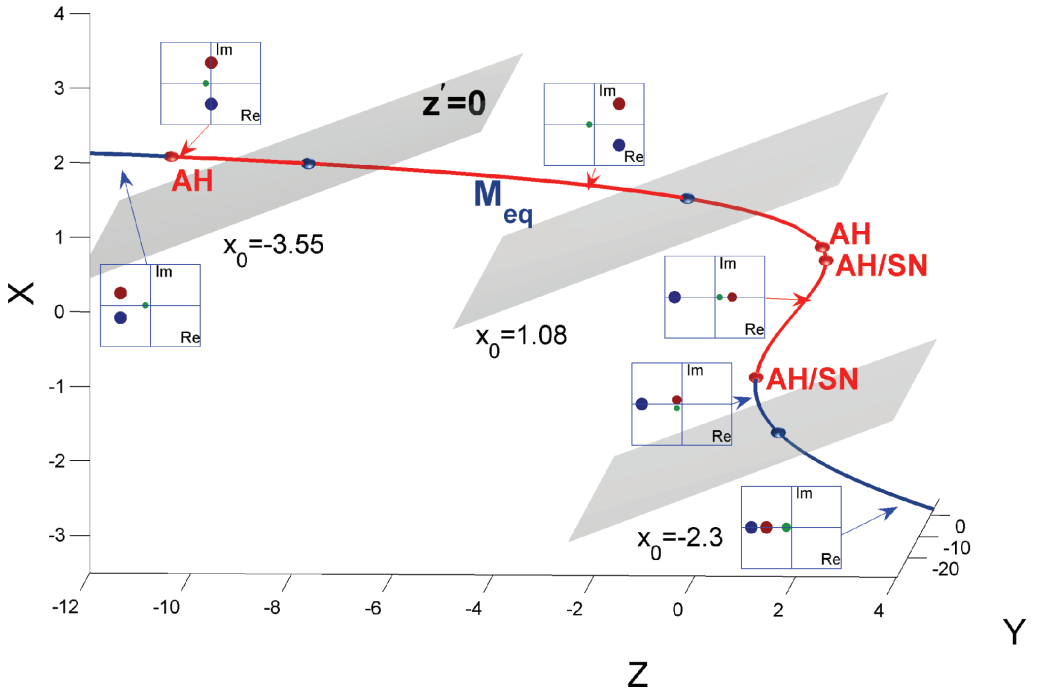

Fig. 5. Intersection point of the branch $M_{\rm eq}$ with the slow nullcline $z' = 0$ yields the equilibrium state of the HR model at given x_0. Insets show the characteristic exponents of the equilibrium state in the complex plane: the red, blue and green points are due to the fast and slow subsystems, respectively.

$M_{\rm eq}$ $z' > 0$ above and $z' < 0$ below the slow nullcline. The corresponding characteristic exponent stays small of order ε. Next, as x_0 is decreased to the value corresponding to $z \sim 11$ of the coordinate of the equilibrium state, it undergoes the supercritical Andronov–Hopf bifurcation in the fast subsystem. At this bifurcation the equilibrium state has a pair of the "fast" complex conjugates crossing the imaginary axis rightwards. As x_0 is decreased further, the next bifurcation on $M_{\rm eq}$ occurs right above the upper fold; it is the same reverse AH bifurcation yet due to the fast subsystem. However, the next two AH bifurcations, labeled in Fig. 5 by AH/SN, are principally different, because they are the result of the mutual interactions between both slow and fast subsystems. For example, consider $x_0 = -2.3$ where there is the stable hyperpolarized equilibrium state with three real distinct eigenvalues, one of which is about $-\varepsilon$. Increasing x_0 elevates the slow nullcline so that the equilibrium state passes throughout the lower fold point and climbs the middle, unstable segment of $M_{\rm eq}$ where it becomes a saddle type with two positive and one negative exponents. One sees that the equilibrium state does persist as the transverse intersection point of both nullclines and hence no saddle-node bifurcation occurs at the transition throughout the fold. This narrows our consideration to the AH bifurcation. Recall that the fold point corresponds to the saddle-node bifurcation in the fast subsystem, where one of two eigenvalues of the equilibrium state vanishes. To find stability of the related equilibrium state in the full system one needs to evaluate the roots of the corresponding characteristic equation. Because the equation is a cubic one, then as x_0 increases the vanishing "fast" root becomes of order of the small one $\sim -\varepsilon$, after that both small ones link and form a double root that converts into a pair of complex, small conjugates. As the equilibrium state is dragged throughout the fold up, this pair crosses the imaginary axis rightward making it unstable, then forms another double root, and finally splits. Moreover, since one of these new positive exponents stays of order of ε, the sum of all three exponents remains always negative. Recall that the saddle value of the equilibrium states in the middle, threshold segment of the manifold $M_{\rm eq}$ is negative in the fast subsystem. Thus, to become a saddle (actually a saddle-focus) around the lower fold on $M_{\rm eq}$ the equilibrium state of the HR model undergoes another, singular perturbed version of the Andronov–Hopf bifurcation. The type of this bifurcation, as well as the stability of the periodic orbit around the bifurcating equilibrium state are

determined by the sign of the Lyapunov coefficient, which is easily evaluated through the polynomial terms of the fast subsystem [Arnold *et al.*, 1994]. It is worth noticing that such a bifurcation leads to the onset of special solutions called *canards* [Callot *et al.*, 1978; Benoit *et al.*, 1981; Krupa & Szmolyan, 2001].

3.2. *Periodic orbits at small ε*

A phase point in the phase space of the HR model at $\varepsilon = 0$ converges to an attractor of its fast subsystem. The attractor is either a stable equilibrium or a stable limit cycle. When this attractor of the fast system is exponentially stable, it depends smoothly on z. By varying z, we obtain a smooth attracting invariant manifold, which can be a space curve like $M_{\rm eq}$ in the phase space, or a two-dimensional cylinder $M_{\rm lc}$ spanned by the limit cycles of the fast subsystem. Moreover, if such a manifold is formed by exponentially stable equilibrium states or limit cycles of the fast subsystem, this manifold is also a center manifold for the system. Since the center manifold persists in a close system, it follows that the smooth attracting invariant manifolds $M_{\rm eq}(\varepsilon)$ and $M_{\rm lc}(\varepsilon)$ will exist too for ε small enough in the full system [Tikhonov, 1948; Pontryagin & Rodygin, 1964; Fenichel, 1979; Shilnikov *et al.*, 1998, 2001].

A phase point of the singularly perturbed slow-fast system at small ε behaves in the following way: within a finite time it arrives into a small neighborhood of either manifolds $M_{\rm eq}$ or $M_{\rm lc}$ so that its z-component stays nearly constant. Then, it drifts slowly along the chosen manifold with rate of change of order ε in z; or meanwhile it will be turning fast around $M_{\rm lc}$.

The slow motion along $M_{\rm eq}$ is either limited to a stable equilibrium state on it, or the phase point reaches a fold from where it jumps onto the slow motion manifold $M_{\rm lc}$, which is the ω-limit set of the outgoing separatrix of the saddle-node equilibrium state of the fast subsystem.

In order to determine the dynamics of the trajectory near the cylinder-shaped manifold $M_{\rm lc}$ we suppose that the equation $\mathbf{x} = \phi(t; z)$ of a $T(z)$-periodic limit cycle of the fast subsystem is known at each z. Plugging this equation into the right-hand side of the slow equation and averaging it over the period of the limit cycle, we arrive at the average equation

$$z' = \varepsilon\langle R(x)\rangle \equiv \frac{\varepsilon}{T(z)}\int_0^{T(z)} R(z, \phi(t; z))dt. \qquad (4)$$

In our specific case, this equation, read as

$$z' = \varepsilon(4(\langle x\rangle - x_0) - z), \qquad (5)$$

gives a first order approximation [Pontryagin & Rodygin, 1964] for the evolution of the z-component of the phase point near the *spiking* manifold $M_{\rm lc}$. Since the shape of the space curve $\langle x\rangle$ is known, see (3) and Fig. 2, we can describe the dynamics of this average equation graphically, using Fig. 6.

One realizes that when $\langle R\rangle$ has a simple zero, the HR model has a single stable periodic orbit on

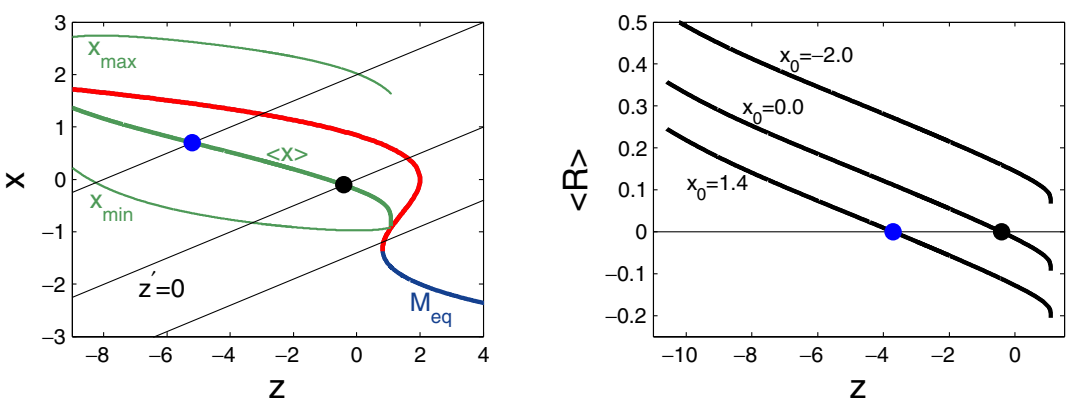

(a) (b)

Fig. 6. (a) The intersection point of the slow nullcline $z' = 0$ with the average branch $\langle x\rangle$ in the (z, x)-projection gives the equilibrium state of the average equation (5). The graph of the function in its right-hand side is shown in (b) for same three different values of the bifurcation parameter x_0 as in (a). A zero of the function is an equilibrium state of (5) that corresponds to a periodic orbit of the HR model on the spiking manifold $M_{\rm lc}$. The stability of the point/orbit in z is determined by whether the graph of $\langle R\rangle$ decreases or not at the given zero. When the function has no zero, like at $x_0 = -2.0$, then the HR model is ready for bursting.

the manifold $M_{\rm lc}$. Its position depends on where the slow nullcline $z' = 0$ cuts $M_{\rm lc}$ through. By changing x_0, we can find such periodic orbits at different locations on the spiking manifold; more specifically around the intersection points of the slow nullcline with the average branch $\langle x \rangle$, as follows from Eq. (5). While staying away from the "homoclinic" edge of $M_{\rm lc}$, the HR model has always the single stable periodic orbit because there is always the single intersection point on the decreasing branch $\langle x \rangle$ with the plane $z' = 0$, see Fig. 7. This stable orbit corresponds to the periodic tonic spiking activity in the model. Its period can be roughly estimated as the reciprocal of the imaginary part of the characteristic exponents of the depolarized equilibrium state of the fast subsystem.

We would like to stress here that the branch $\langle x \rangle$ connects the AH and homoclinic bifurcation, and thus the ranges of the variables in Eq. (5) are set accordingly. Note here that if the slow equation were *not* linear in x, then the crossing point of this average branch and the slow nullcline would *no longer* be the "center of gravity" of the selected periodic orbit; since $\langle x^2 \rangle \neq \langle x \rangle^2$ in general. This fact has been often ignored in studies of various neuronal models with nonlinear slow nullclines. Instead one has to examine the so-called average slow nullclines introduced originally in [Cymbalyuk & Shilnikov, 2005; Shilnikov *et al.*, 2005; Shilnikov & Cymbalyuk, 2005] that give the correct information for localizing periodic orbits and for detecting their bifurcations, local and global, on the spiking manifold $M_{\rm lc}$.

In the end we would like to make another important conclusion: a simple, round periodic solution of the HR model at small ε is known to be ε-close to the spiking manifold $M_{\rm lc}$ introduced from the fast subsystem. Its location on $M_{\rm lc}$ depends on x_0. By varying x_0 we make it slide along $M_{\rm lc}$. Thus, to localize the manifold $M_{\rm lc}$ we continue perimetrically the corresponding branch foliated by the periodic orbits of the full system instead. This means that to localize and examine both slow motion manifolds $M_{\rm eq}$ and $M_{\rm lc}$ in a given model one *needs no slow-fast decomposition* but continue the corresponding branches of equilibria and periodic orbits of the given system. Again, this approach works especially well for the high-dimensional models [Shilnikov & Kolomiets, 2008] including the 14D canonical leech heart

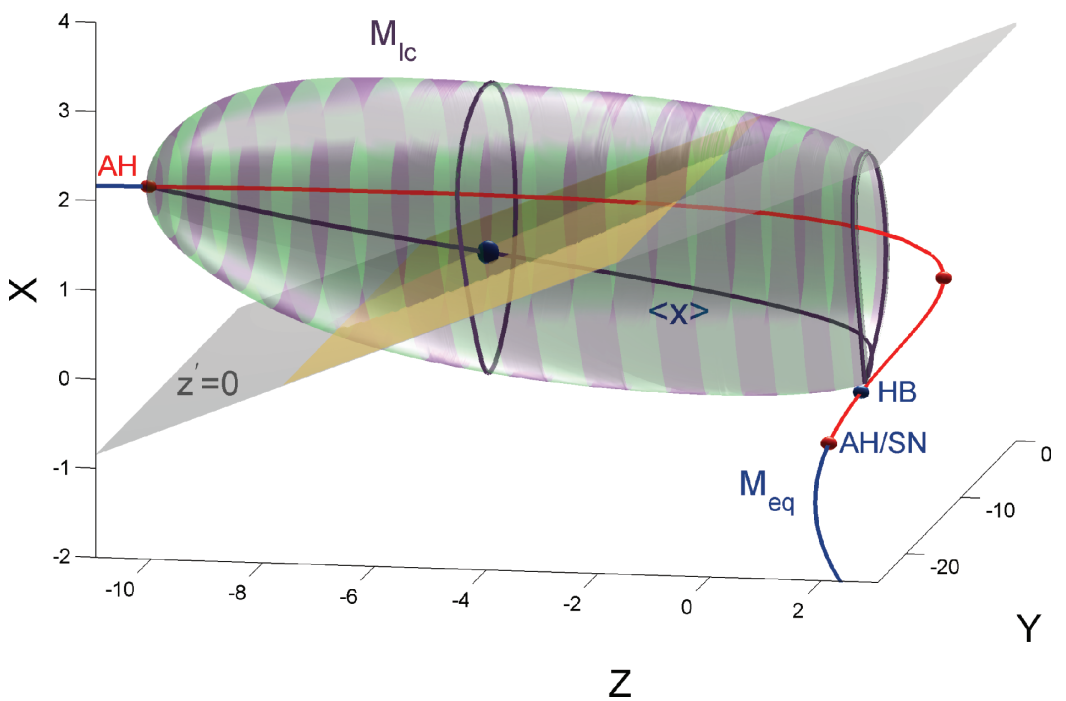

Fig. 7. 3D version of Fig. 6(a). The blue point is the center of gravity of the stable periodic orbit of the HR model, which is depicted on the tonic spiking manifold $M_{\rm lc}$ at $x_0 = 1.8$. It is located around the intersection point of the slow nullcline $z' = 0$ with the average space curve $\langle x \rangle$. The phase point, while turning around $M_{\rm lc}$, is pushed by the flow rightward as long as it is above the nullcline where $z' > 0$, and pushed back to left when it goes below the nullcline. When these opposite forces are canceled out, the phase point spins around the "center of the gravity", i.e. stays on the desired periodic orbit.

interneuron and the 13D cortical neuron models (for example).

4. Bursting as a Slow-Fast Phenomenon

The HR model describes one of the most typical configurations of slow manifolds needed for square-wave bursting to occur naturally in various neuron models of the Hodgkin–Huxley type [Bertram, 1993; Chay, 1983, 1985; Butera, 1998], see Fig. 1. First of all, a model needs the distinct Z-shape for the quiescent manifold. Its lower (stable) branch corresponds to a hyperpolarized quiescent state of the neuron. The upper, depolarized branch is unstable in this configuration and surrounded by the spiking manifold $M_{\rm lc}$ foliated by the stable limit cycles of the fast subsystem. This manifold terminates through the homoclinic bifurcation that occurs in the fast subsystem. Between the hyperpolarized fold and this homoclinic point, the system has a hysteresis to have bursting generated. In the bursting regime, the phase point of the HR model switches repeatedly between the spiking $M_{\rm lc}$ and quiescent $M_{\rm eq}$ manifolds after it reaches their ends. In addition, both manifolds must be transient for the passing solutions of (1). For $M_{\rm eq}$ this means that the slow nullcline does not get through it to the right from the hyperpolarized fold point, but goes across the middle, saddle branch of $M_{\rm eq}$ below $M_{\rm lc}$. The latter condition guarantees that $M_{\rm lc}$ is also transient for the trajectories of the model that coil around it while translating slowly towards its edge corresponding to the aforementioned homoclinic bifurcation. Thus, the rapid jump from the lower point on $M_{\rm eq}$ towards $M_{\rm lc}$ indicates the beginning of the spiking period of a burst followed by the interburst phase when the phase point drifts slowly along $M_{\rm eq}$ towards the fold, onto which it lands right after the homoclinic bifurcation. The number of complete revolutions of the phase point around the spiking manifold $M_{\rm lc}$ gives the number of spikes within a burst, see Fig. 1, as well as Fig. 8. Thus, the described configuration of slow manifolds serves as a geometric paradigm for bursting [Rinzel 1985; Rinzel & Ermentraut, 1989; Bertram *et al.*, 2000; Izhikevich, 2000].

It is evident that when there is a periodic orbit on the spiking manifold like in Fig. 7, then the model fires tonically instead. Below we will discuss the way the tonic spiking activity transforms into bursting as the parameter x_0 is decreased. Clearly this is accompanied with the disappearance of this periodic orbit. We will consider examples of such natural causes in the HR model itself, as well as some other peculiar mechanisms that are only realized in the model after its slow equation is modified accordingly.

We can see that the number of turns, or spikes per burst, that the phase point makes around $M_{\rm lc}$ is determined by the time it needs to drift from the hyperpolarized fold on $M_{\rm eq}$ to the homoclinic edge on $M_{\rm lc}$. In turn, this time, or the burst duration, is evaluated from the averaged equation (5). Putting simply, it depends how far the graph of $\langle R\rangle$ in Fig. 6(b) is above zero, or is determined by the distance between the slow nullcline $z' = 0$ and the branch $\langle x\rangle$. By the particular construction of the model, function $\langle R\rangle$ can stay positive but close to zero only in the vicinity of the homoclinic bifurcation. This implies that with the given linear slow nullcline there are no effective mechanisms of regulation of bursting rhythmogenesis in the model, unless its shape is altered in a way, or differently to, what we suggest in the last section of this paper. There is another trivial solution for regulation of the temporal characteristics of the bursting activity as decreasing the small parameter ε in order to prolong the spiking period of the bursts. However, there is a price to pay for that as well, since the interburst interval will increase proportionally too.

In conclusion, we point out that other types of bursters, like plateau-shaped oscillations are available in the HR model as well. This is achieved not through an interplay between its subsystems, but solely via changes in the fast subsystem, see Figs. 2(a) and 2(d). Moreover, at the transition one can observe chaotic alteration between bursters of both types. The new bursters have duration twice as long; this fact was interpreted in [Bazhenov *et al.*, 2000] as the result of inhibitory synaptic couplings between HR neurons. Indeed, this is merely an artifact of the fast subsystem of the model and the fine choice of the polynomial terms on its right-hand side.

Recall that the terminal phases of the slow motion manifold $M_{\rm lc}$ are different for various values of the parameter a. If $a = 1$, then this is the homoclinic loop of the saddle, however if $a = 1.66$, this is the reverse AH bifurcation. One can see from Fig. 4 that at some intermediate value $a = 1.2133$, the z-passway becomes tangent to the homoclinic curve HB in the (z, a)-parameter plane. This results in that the branch $M_{\rm lc}$ is no longer transverse, but

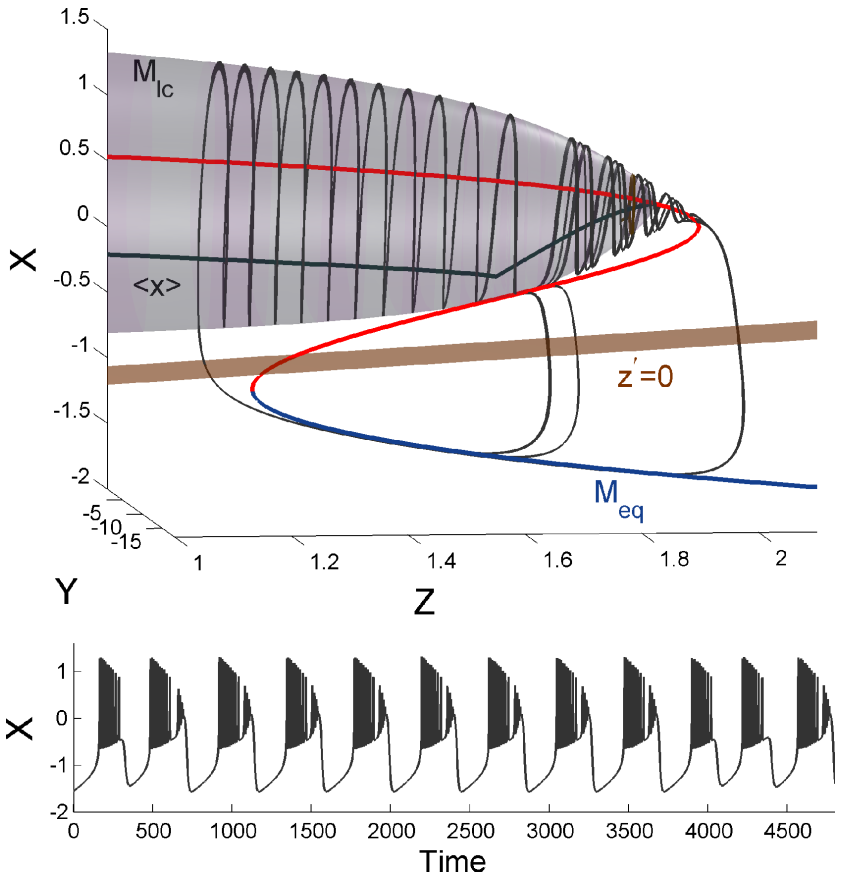

Fig. 8. Square-wave bursting (Fig. 1) becomes a plateau-like one after the spiking manifold $M_{\rm lc}$ becomes tangent to the middle, saddle branch of $M_{\rm eq}$ and terminates further through the reverse Andronov–Hopf bifurcation on the depolarized branch of $M_{\rm eq}$. The forms of the bursts and their durations in the wavetrain alter chaotically. Observe the window in bursts when the phase point follows this middle branch after it gets close to the saddle point.

becomes cylinder shaped tangent to the saddle branch of $M_{\rm eq}$ at a joint point. Figure 8 shows the two types of the alternating bursting in the HR model due to this fact. The transition can lead to a very peculiar property of the square-wave bursters, namely that when the phase point turning around $M_{\rm eq}$ happens to pass close by the saddle of the fast subsystem, it can follow the saddle branch as far as to the upper, depolarized fold point. While doing so the phase point shall eventually make sporadic fast jumps down or up onto the depo- and hyperpolarized branches of $M_{\rm eq}$. Indeed this trajectory behavior presents another type of canards being the special solutions that follow unstable branches, as they are broadly understood nowadays.

5. Poincaré Mapping

In this section we start examining the transition from the tonic spiking activity to square-wave bursting in the model and reveal the global bifurcations underlying it. The feature of the transition in this [Wang, 1993], as well as in many other HH models is that it occurs within narrow (in the parameter sense) windows of chaos [Terman, 1992]. Therefore, we need tools more advanced than the average equation (5) to understand chaotic dynamics in the model. While explaining well the stability and local bifurcations, such as saddle-node, of periodic orbits, the average equation becomes less useful for other bifurcations including period-doubling. Instead we show the way this single equation can be converted into a 1D Poincaré mapping [Shilnikov *et al.*, 2001; Shilnikov *et al.*, 2005; Medvedev, 2006] that handles period-doubling bifurcations exceptionally well.

The Poincaré mapping technique is proven to be a highly effective method in the theory of bifurcations, as well as in many other areas of dynamics. In the slow-fast systems framework such a mapping is derived as the composition of several consecutive segments of Poincaré mapping describing different

stages of the orbit behavior. So, the Poincaré mapping corresponding to the slow motion is evaluated through (5), whereas one corresponding to the fast jump is, up to the first order in ε, determined by the integration of the fast subsystem at the critical value. Routinely, the most technical part is computing the Poincaré mapping near the transitions between slow and fast motion branches, where the so-called "blow-up" methods [Dumortier & Roussarie, 1996; Krupa & Szmolyan, 2001] or the rescaled normal form methods are to be employed in addition to computations similar to those performed in [Terman, 1992; Deng & Hines, 2002]. This combined technique is, in fact, quite close to that used in the study of the first-return maps for homoclinic bifurcations [Shilnikov *et al.*, 1998, 2001], where the averaging technique was enhanced to derive 1D Poncaré mappings to examine the blue sky bifurcations in the slow fast systems [Shilnikov *et al.*, 2001; Shilnikov *et al.*, 2005]. The approach first introduced in [Shilnikov *et al.*, 2001; Shilnikov *et al.*, 2005c] lets one define a 1D Poincaré mapping on some space curve $m_{\rm lc}$ on the spiking manifold $M_{\rm lc}$, which is transverse to the oscillatory orbits of the system; for example, at their minima where $x' = 0$. The mapping is then recast as

$$z_{n+1} = z_n + \varepsilon \langle R(z_n, x_0) \rangle T(z_n) + o(\varepsilon). \qquad (6)$$

Formally, this is the average differential equation (5) rewritten in the form of the difference one with the time steps equal to the periods of the orbits forming $M_{\rm lc}$ in the unperturbed system.

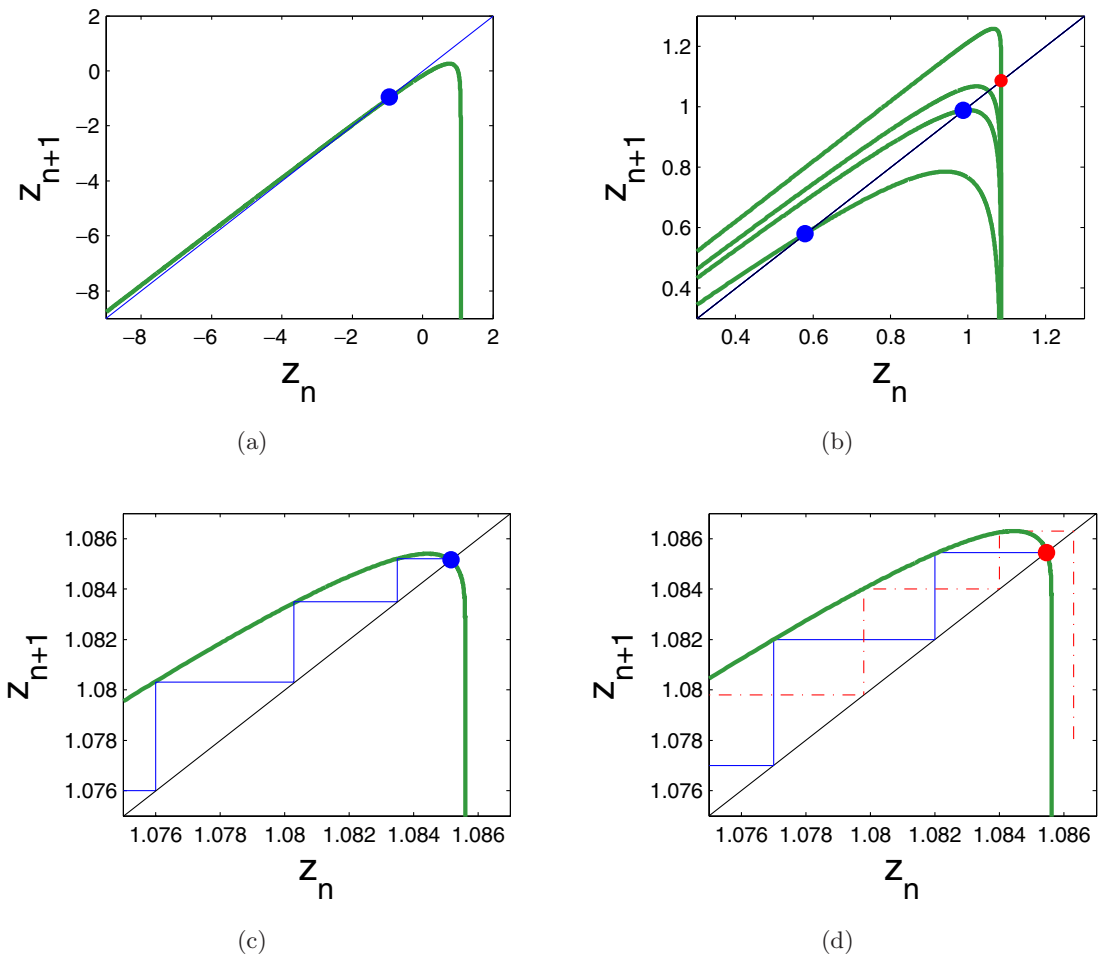

Fig. 9. 1D Poincaré mappings for $\varepsilon = 0.01$, which is chosen to be quite large for visual clarity; at smaller values the mapping graph is indistinguishable from the bisectrix. (a) The Poincaré mappings at $x_0 = 0.5$: its stable fixed point corresponds to the stable periodic orbit that flows into the homoclinic loop (corresponding to the vertical slope) of the saddle as x_0 is decreased further. (b) Mapping at $x_0 = (-0.5, -0.8, -0.9, -1.0)$: as its graph becomes steeper the fixed point loses stability through the period-doubling bifurcation. Inset (c) shows transient iterates converging to the yet stable fixed point. After it becomes unstable, the system may exhibit bursting with unpredictable numbers of spikes per bursts when the bursting orbit comes close by this repelling fixed point (d).

Specifically, its primary feature is based on the dependence of the period of the orbit on z: it grows with no upper bound when the orbit flows into the homoclinic loop.

Let us examine some properties of the Poincaré mapping (6). The first one is obvious: its fixed point is the same zero of function $\langle R\rangle$ whose graph is shown in Fig. 7. One sees that the graph of the mapping is primarily determined by the product of $\langle R\rangle$ (from Fig. 6) and the period $T(z)$ (from Fig. 3), weighted by the small parameter. The period is known to increase logarithmically fast as $-\ln(z_h - z)$ at homoclinic bifurcations of saddles; here z_h is the coordinate of the homoclinic saddle in the HR model.

Let us discuss the evolution of the Poincaré mappings corresponding to the HR model as x_0 is decreased for $\varepsilon = 0.01$, see Fig. 9. Its single fixed point, stable first, loses stability through the period-doubling bifurcation. This occurs when it is moved closer to the steeper section of the map whose vertical segment is to be interpreted as the homoclinic loop of the saddle. Recall that the period T becomes infinitely large while the function $\langle R\rangle$ remains finite and takes on negative values prior to the homoclinic bifurcation. This is imperative as it makes the graph of the mapping become concave down and have an infinitely steep negative slope as z_n approaches the homoclinic value.

Right after the period-doubling bifurcation, the model fires spikes that can be called duplets, then quadruplets after the second period-doubling bifurcation, and so forth, before its dynamics becomes chaotic with irregular bursts with unpredictable number of spikes. This number increases if the bursting orbit passes close by the fixed point. Note that unlike the classical parabola case, the period-doubling cascade in this case may be finite before the system starts firing bursts.

The period-doubling cascade, complete or not, is a common phenomena at the transition between tonic spiking to bursting activities in neuronal models that fall into the square wave bursters category [Wang, 1993; Chay, 1983, 1985; Rowat *et al.*, 2004; Medvedev, 2006]. We stress that its cause is not only limited to the case of the terminating homoclinic bifurcation [Shilnikov & Rulkov, 2003; Deng, 2004]; so for example, the complete period-doubling cascade preceding the emergence of busting in the reduced model of the heart interneuron [Cymbalyuk & Shilnikov, 2005] is due to the fold on the tonic spiking manifold $M_{\rm lc}$ instead, which could lead to a torus bifurcation [Shilnikov & Rulkov, 2004] should the fast subsystem be of a higher (3 or more) dimension [Cymbalyk & Shilnikov, 2005; Kramer *et al.*, 2008].

6. Homoclinic Bifurcations

We said earlier that the formation mechanism of square-wave bursting [Rinzel, 1985; Bertram *et al.*, 2005], or alternatively the "fold/homoclinic" bursting [Izhikevich, 2001] is directly related to the homoclinic bifurcation that occurs in the slow subsystem of the HR model at some z_h. An associate bifurcation shall occur in the whole model at the transition between tonic spiking and bursting activities at some critical value x_0 when the slow nullcline crosses the branch $M_{\rm eq}$ at the saddle with the corresponding coordinate z_h. From the general point of view, this is a special, degenerate type of a homoclinic bifurcation of codimension-2 called an orbit-flip, see the detailed description of cod-2 homoclinic bifurcations in [Shilnikov *et al.*, 2001] the references therein. The methods and results from [Shilnikov, 1986, 1993; Robinson, 1989; Rychlik, 1990; Deng, 1993; Shilnikov *et al.*, 1993] can be applied in the straightforward manner to study homoclinic bifurcations in slow-fast systems too. The features of this homoclinic bifurcation include and therefore explain well period-doubling bifurcations and the onset of chaotic dynamics that underly transitions from periodic tonic spiking to bursting in many models of square-wave bursters.

Let us begin with the planar case $\varepsilon = 0$, where the stable periodic orbit becomes a homoclinic loop of the saddle equilibrium state. Denote its characteristic exponents by $-\lambda_1 < 0 < \lambda_2$; they must meet a single condition: the saddle value $\sigma_1 = -\lambda_1 + \lambda_2 < 0$ or index saddle index $\nu = |\lambda_1|/\lambda_2 > 1$ [Shilnikov *et al.*, 1998, 2001]. Bifurcations of the nonwandering set, including periodic orbits, near the loop of the saddle are examined with the use of a simple 1D Poincaré mapping:

$$\overline{x} = \mu + Ax^{\nu}, \tag{7}$$

where the condition on a separatrix coefficient $0 < A < 1$ holds true in a plane; here μ is a small bifurcation parameter controlling locally, near the saddle, the distance between its stable and unstable manifolds. Leontovich [1951] showed that when the saddle is not resonant, i.e. $\sigma \neq 0$ (or $\nu \neq 1$), then this codimension-1 homoclinic bifurcation generates a single limit cycle in a plane. This cycle is

stable if $\sigma < 0$. Let us examine the homoclinic saddle in the whole HR model for small $\varepsilon \neq 0$. As we said earlier (to recall, see Fig. 5) that in addition to the "fast" unstable characteristic exponent, the saddle will get another one $\lambda_3 \simeq \varepsilon$. This makes the saddle of topological type $(1, 2)$ in R^3; i.e. it has an 1D stable W^s and a 2D unstable manifold W^u. Shilnikov [1965] showed that in R^3 and higher, a codimension-1 homoclinic bifurcation generating a single periodic orbit must meet additionally two more conditions: (1) as before the saddle value $\sigma = -\lambda_1 + \min \lambda_{2,3} \neq 0$; (2) the stable separatrix comes back to the saddle as $t \to -\infty$ along the leading direction determined by $\min \lambda_{2,3}$; and finally (3) the separatrix coefficient $A \neq 0$. The last condition is interpreted as follows: the closure of the 2D unstable manifold is homeomorphic to a cylinder if $A > 0$, and to a Möbious band if $A < 0$. This implies also that the new born periodic orbit will have a pair of positive or negative Floquet multipliers, respectively. Further details on homoclinic bifurcations can be found in [Shilnikov *et al.*, 2001].

Whenever one of the above conditions is not fulfilled, the homoclinic bifurcation becomes degenerate, and its codimension increases to two. So, for example the unfolding of the homoclinic resonant saddle includes a saddle-node bifurcation of periodic orbits [Shilnikov, 1986, 1992; Nozdracheva, 1992; Chow *et al.*, 1990].

A violation of the second or the third condition in the case where $\sigma > 0$ leads to the bifurcations called the inclination-flip and the orbit-flip, respectively. Both act similarly, and therefore

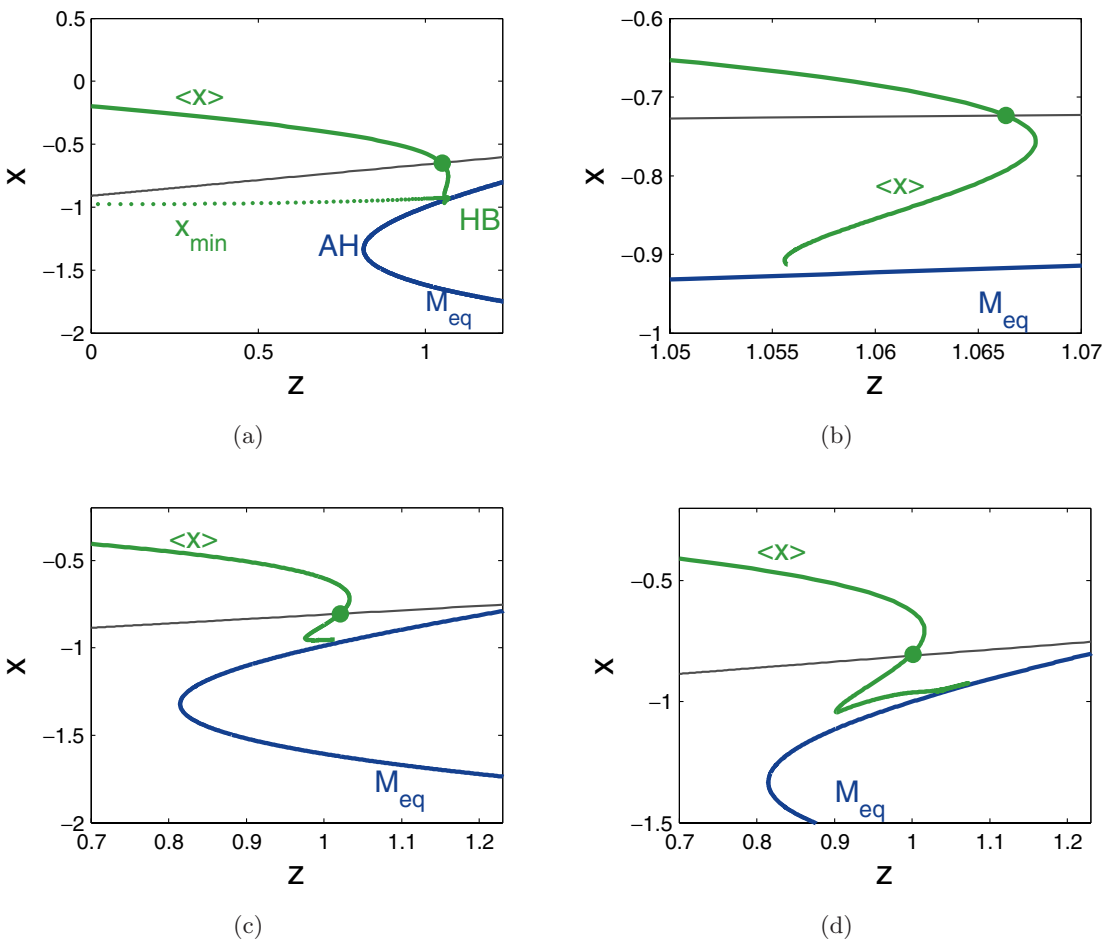

Fig. 10. (a) The average branch $\langle x \rangle$ of the spiking manifold $M_{\rm lc}$ plotted against $\langle z \rangle$ for (a) $\varepsilon = 0.001$, (b) $\varepsilon = 0.004$, (c) $\varepsilon = 0.008$ and (d) $\varepsilon = 0.0127$. The formation of the fold on $\langle x \rangle$ can be misinterpreted as the saddle-node bifurcation on $M_{\rm lc}$; indeed this is the way this branch is projected onto the (z, x)-plane when the homoclinic orbit undergoes an orbit-flip bifurcation. When the intersection point of the slow nullcline with $\langle x \rangle$ goes below the fold point, the corresponding periodic orbit undergoes a period-doubling bifurcation.

have a similar unfolding including period-doubling, saddle-node and secondary homoclinic bifurcations in addition.

It is clear that when ε becomes nonzero remaining small, the leading unstable direction of the saddle changes, so that the 1D stable separatrix begins returning to the equilibrium state along the direction tangent to the branch of $M_{\rm eq}$ instead in the backward time. Thus, $\varepsilon = 0$ corresponds to a singular orbit-flip bifurcation. Figures 10 and 12 reveal the transformation stages of the homoclinic loops as ε increases from zero. Observe that the projections of $\langle x \rangle$ in Fig. 10 can be misinterpreted as new folds on the tonic spiking manifold $M_{\rm lc}$, which correspond to new saddle-node bifurcations of the limit cycles in the fast subsystem.

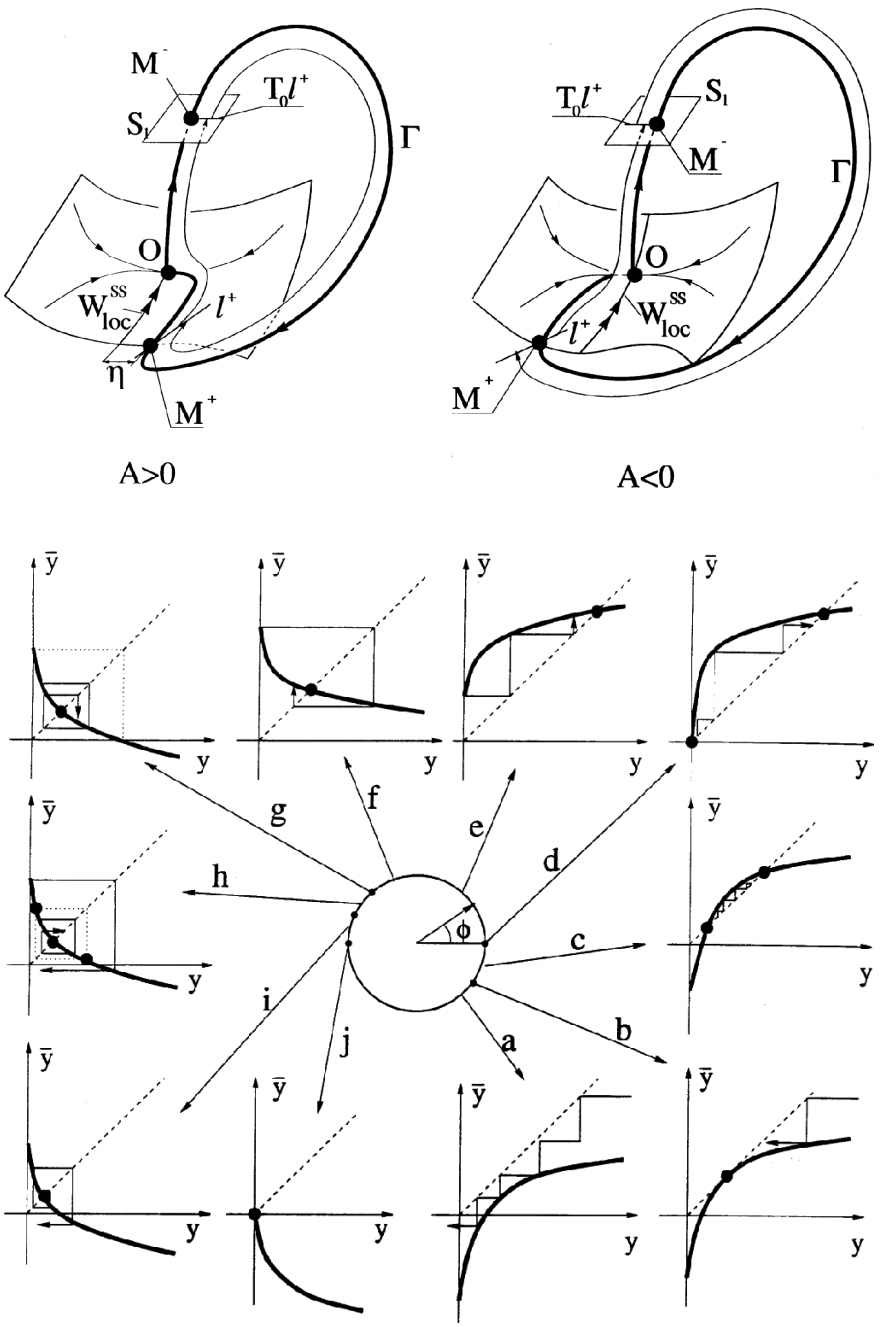

Fig. 11. Orbit-flip bifurcation: the unstable separatrix enters the saddle from either side of the strongly stable (nonleading) manifold W^{ss} in the oriented, $A > 0$, and nonoriented, $A < 0$, cases. Bifurcation unfolding in the corresponding Poincaré mapping showing the saddle-node, period-doubling and secondary homoclinic bifurcations. From [Shilnikov *et al.*, 2001].

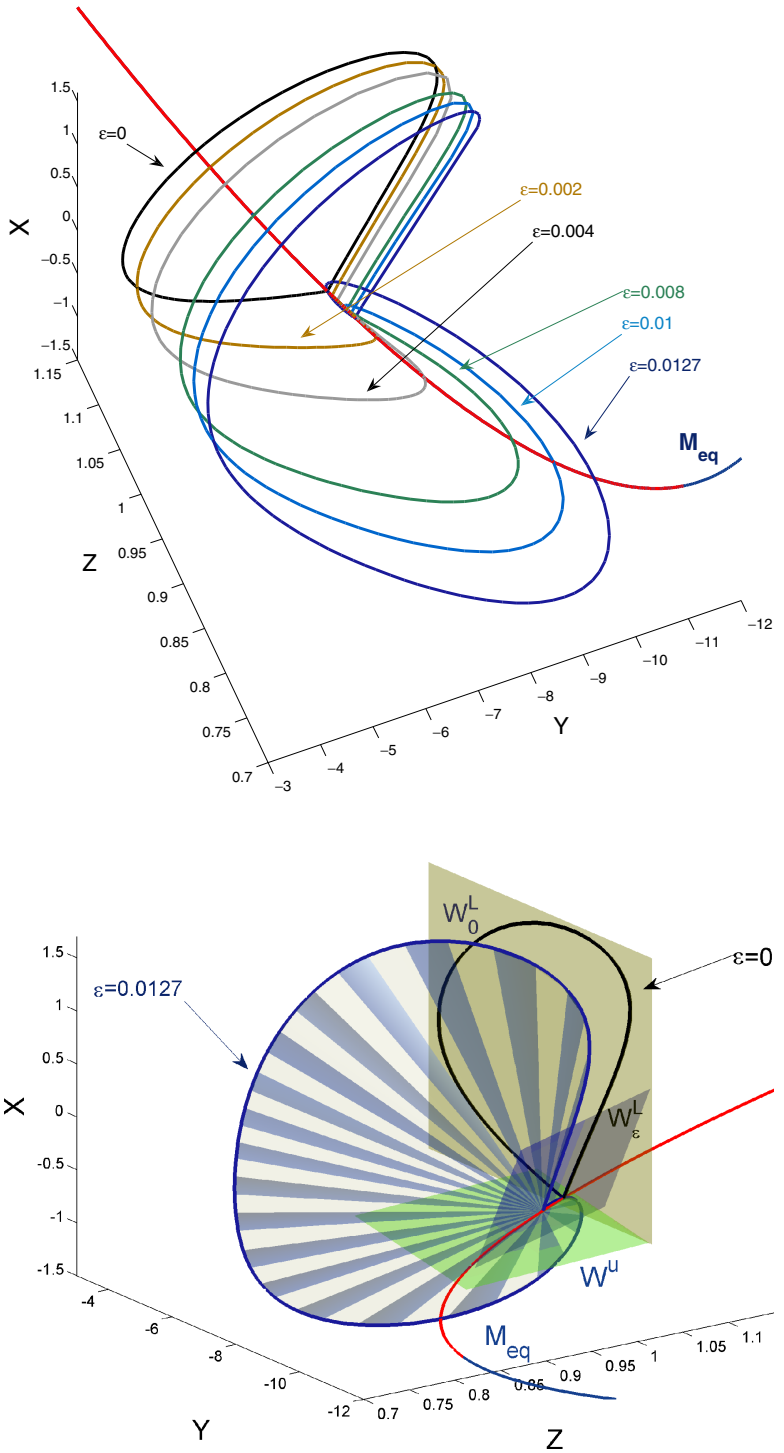

Fig. 12. (Top) Evolution stages of the (x, y)-"flat" homoclinic loop of the saddle point at $\varepsilon = 0$ as the small parameter increases from 0.002, 0.004, 0.008, 0.001 through 0.0127. The homoclinic orbit undergoes an orbit-flip bifurcation that changes the way 1D stable separatrix enters the saddle in its 2D unstable manifold W^u as $t \to -\infty$: now the stable leading unstable direction tangent to M_{eq} is determined by the characteristic exponent due to the small parameter. Here W_0^L stands for the leading subspace spanned by the leading unstable and stable eigenvectors of the saddle in the unperturbed perturbed model.

Let us next consider the above Shilnikov theorem applied to the HR model when it is away from the orbit-flip bifurcation. In order to determine the stability of the periodic orbit emerging from the homoclinic loop, we have to reverse the time in the system. After that the saddle becomes of type (2, 1), i.e. has the 1D unstable manifold that comes back to the saddle along the direction tangent to

the middle branch of $M_{\rm eq}$. The first saddle value σ is then evaluated as $\lambda_1 + \varepsilon > 0$; moreover the positiveness of the second saddle value $\sigma_2 = \sigma + \lambda_2$ means the expansion of 3D phase volumes. Thus, only a saddle periodic orbit may come out of such a homoclinic loop. This periodic orbit remains of the saddle type as well after the time is changed back. So, one may wonder how the orbit, being stable away from the homoclinic saddle, becomes of the saddle type prior to the bifurcation? One can see from Fig. 10 that the intersection point of the average branch $\langle x \rangle$ with the slow nullcline persists all the way through the homoclinic bifurcation. This rules out a saddle-node bifurcation from consideration. Then, our choice narrows down to a period-doubling bifurcation, which is confirmed by the mappings in Fig. 8. Hence, the periodic orbit loses stability via a period-doubling bifurcation (Fig. 9) right when the intersection point goes through the fold point in Fig. 10. By repeating the arguments, we assert that the new born stable period-2 orbit may not vanish in a similar homoclinic bifurcation, and then should soon undergo another period-doubling bifurcation as well, and so forth. This observation explains well the short period-doubling cascade frequently observed at the transition from tonic spiking to bursting through the homoclinic bifurcation.

One can see from Figs. 2(c) and 2(d) and 10, for example, that the average branch $\langle x \rangle$ that used to terminate on $M_{\rm eq}$ with a vertical tangent at $\varepsilon = 0$, becomes tangent to $M_{\rm eq}$ for $\varepsilon \neq 0$. Moreover, it may enter the saddle equilibrium state swinging from either side. In terms of Eq. (7) (see 8), this means changes of the sign of the separatrix value A between the oriented "+" to non-oriented "−" cases. Figure 12 illustrates this point: the flat homoclinic orbit lying in the plane $z = z_h$ becomes a space curve that enters the saddle as $t \to -\infty$ being tangent to $M_{\rm eq}$ for $\varepsilon = 0.0127$.

To conclude, we conjecture that the unfolding of this singular orbit-flip bifurcation can be adequately explained in terms of the following 1D Poincaré mapping [Shilnikov *et al.*, 2001; Shilnikov & Turaev, 2008]

$$\overline{x} = \mu \pm \varepsilon x^{\varepsilon} + A x^{\nu}, \tag{8}$$

where the new small term is due to the singular perturbation, while the second one is a relic from the fast subsystem. Because of the ± sign, the unfolding of this homoclinic bifurcation contains three bifurcation curves corresponding to period-doubling, saddle-node and secondary homoclinic bifurcations [Shilnikov *et al.*, 2001]. A feature of this singular mapping is chaotic dynamics as depicted in Fig. 13. This bifurcation is a first step toward the Shilnikov saddle-focus that would occur should the saddle point get pushed down closer to the hyperpolarized fold point on $M_{\rm eq}$ [Deng & Hines, 2002].

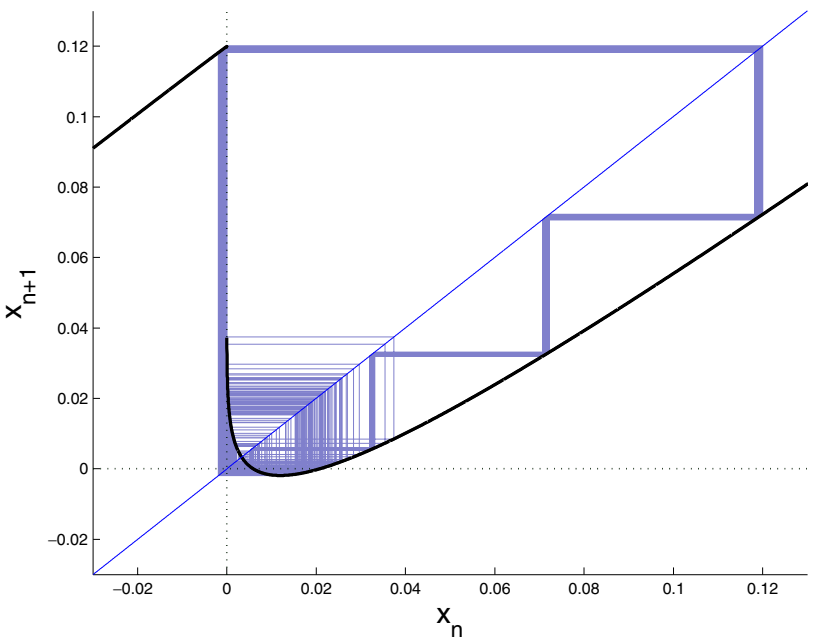

Fig. 13. Chaos in the 1D Poincaré mapping (8). The left branch is due to the reinfection mechanism via the low hyperpolarized branch forming the interburst periods. One sees from the figure that "regular" four spikes burst becomes chaotic when the phase point comes close to the unstable fixed point.

7. Alien Bifurcations

7.1. *Melting manifold*

Let us get back to Fig. 1 showing a typical square-wave bursting in the HR model at $\varepsilon = 0.002$. One sees that this small parameter gives about five spikes per burst, which is the number of complete revolutions of the phase point around $M_{\rm lc}$ while its z-component increases from the low hyperpolarized fold on $M_{\rm eq}$ through the homoclinic wedge of $M_{\rm lc}$. One would expect that increasing ε should decrease the flight time between these break points. This seems true, however, only far from the homoclinic bifurcation underlying the transition between bursting and tonic spiking. Indeed, at higher values of ε the homoclinic orbit-twist makes $M_{\rm lc}$ look as it gets some kind of a "chin" beyond the terminal point, see Fig. 14. This leads to the onset of even more developed chaos induced by this bifurcation, where bursting acquires more spikes when the phase point gets closer to the now unstable spiking periodic orbit (Fig. 11). A further increase of ε leads to even more paradoxical result, namely, chaotic bursting gains subthreshold oscillations, see Fig. 15. To figure out their cause we apply the parameter continuation technique to determine the spiking manifold $M_{\rm lc}$. It is shown in Figs. 14 and 15. We call it a "melting" manifold in the analogue with the painting by S. Dali. The cause for the drastic change of the shape of $M_{\rm lc}$ is similar to that generating the plateau bursting in Fig. 9, namely: at $\varepsilon = 0.02$ the x_0-parameter pathway no longer crosses the homoclinic bifurcation curve in the parameter space that was used to terminate the branch of the periodic orbits. Instead now $M_{\rm lc}$ ends up through the Andronov–Hopf bifurcation around the lower fold of $M_{\rm eq}$ (see the bifurcation diagram in Fig. 6 and the discussion there). This AH bifurcation is the result of the interaction of the dynamics of both fast and slow subsystems. Dynamically, this bursting activity has quite large amplitude subthreshold oscillations that, however, in the projection onto the x-variable have a rather small magnitude since the eigenspace, or a local central manifold on which this AH bifurcation takes place is orthogonal to the x-axes, as depicted in Fig. 15. Note that this kind of bursting is nowadays referred often to as mixed mode oscillations.

7.2. *Blue-sky catastrophe*

Since the slow nullcline of the HR model is linear in both x and z, then its graph is a plane in the 3D phase space of the model. Due to this linearity, search for periodic orbits of the model presents no difficulty: the intersection point of the nullcline with the space average curve $\langle x \rangle$ yields the gravity center of the desired orbit. Since $\langle x \rangle$ beginning from the AH bifurcation descends toward the terminal point due to the homoclinic bifurcation, there is always the single intersection point. This rules out a chance for the saddle-node bifurcation on the tonic spiking manifold $M_{\rm eq}$ that might have led to very peculiar bifurcations in the model and could have implied long bursting and the co-existence of tonic spiking or depolarized silence and bursting activities in the model [Cymbalyuk & Shilnikov, 2005; Shilnikov *et al.*, 2005; Shilnikov & Cymbalyuk, 2005].

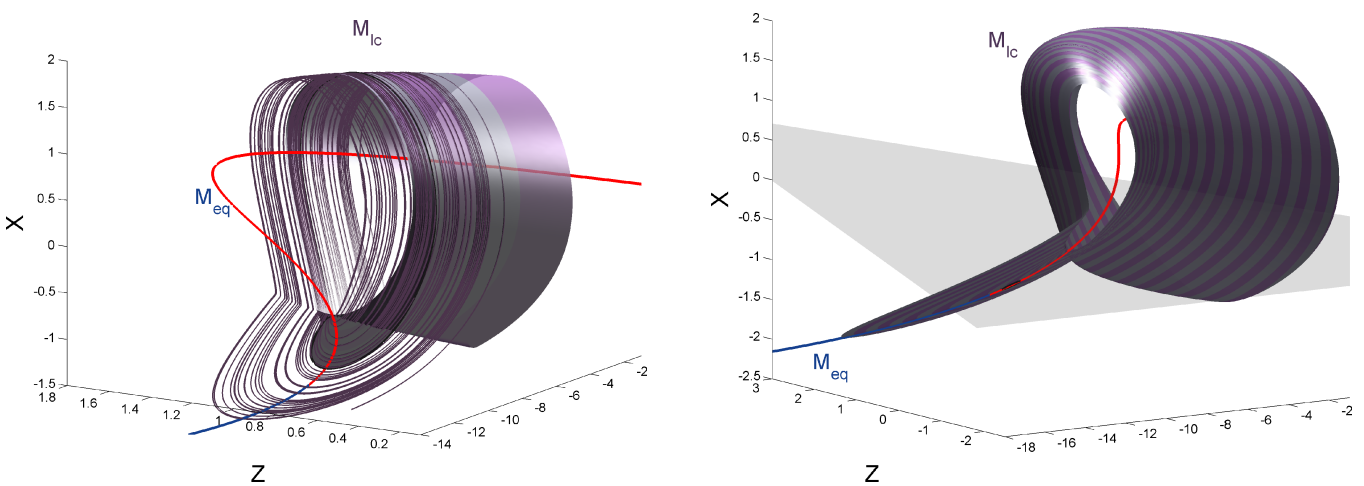

Fig. 14. (Left) Homoclinic chaotic bursting in the model at $\varepsilon = 0.0127$. (Right) "Melting" tonic-spiking manifold in the HR model at $\varepsilon = 0.02$ terminates through the *canard*-initiating AH bifurcation near the lower fold.

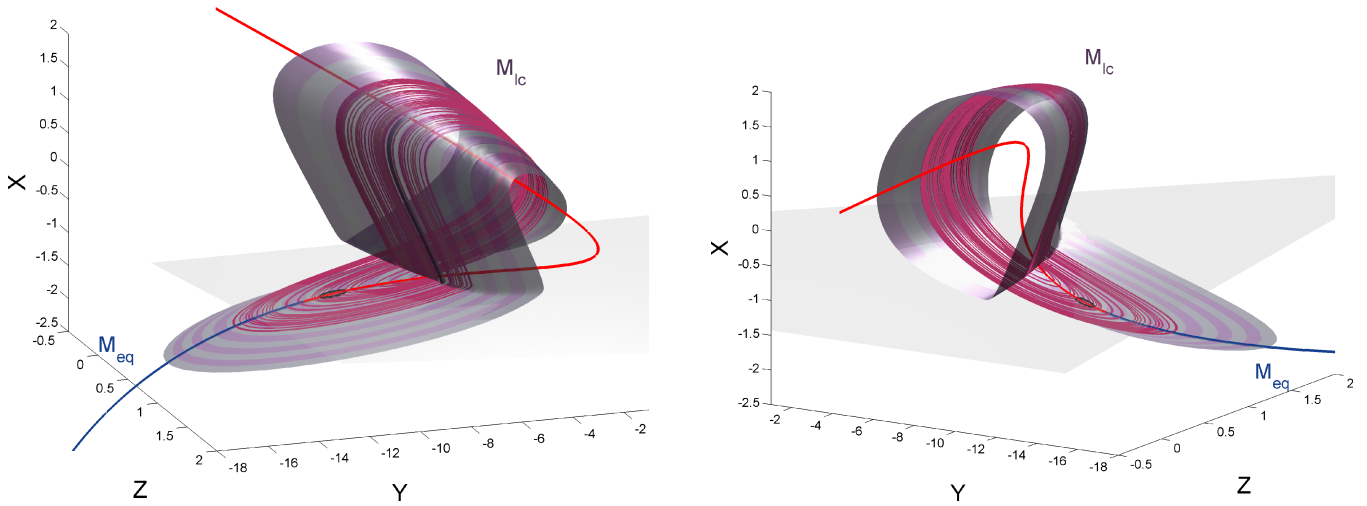

Fig. 15. Chaotic bursting due to the interaction of the slow and fast time dynamics near the AH bifurcation.

The first mechanism describing a reversible and continuous transition between spiking and bursting in neuron models in the given context is based on a codimension-one bifurcation known as the *blue-sky catastrophe* [Shilnikov & Turaev, 1997, 2000; Shilnikov *et al.*, 2001]. The rigorous proofs and three scenarios of the blue-sky catastrophe in singularly perturbed systems are given in [Shilnikov *et al.*, 2005c].

The blue-sky catastrophe shall occur in the HR model if we alter the linear shape of the slow nullcline by changing the slow equation

$$\dot{z} = \varepsilon \left(s(x - x_0) - z - \frac{\alpha}{(z - z_0)^2 + 0.03} \right), \quad (9)$$

so that the slow nullcline gains a "hump", see Fig. 16; here α regulates its height, while z_0 determines its location along the z-axis. By varying α we control the saddle-node bifurcation occurring when the hump crosses the average branch $\langle x \rangle$ (since the hump is set narrow enough). By elevating the slow nullcline, we obtain two new intersection points and hence two new periodic orbits on the spiking manifold $M_{\rm lc}$. Recall that $M_{\rm lc}$ is stable in the (x, y)-subspace, because it is comprised of the stable limit cycles of the fast subsystem. As far as the stability of these orbits in z is concerned, one is stable, and the other is unstable. This makes the first periodic orbit stable in the phase space, while the second one is of the saddle type, with some 2D stable and unstable manifolds. Locally, $M_{\rm lc}$ represents the unstable manifold of the saddle orbit. Clearly, when the hump is lowered, leaving no intersection points, the manifold $M_{\rm lc}$ is ready for bursting.

The local saddle-node bifurcation of the periodic orbits constitutes only the first component in the blue-sky catastrophe in slow-fast systems. A simple saddle-node periodic orbit in $\mathbb{R}^3$ has two unique manifolds. The strongly stable manifold W^{ss} divides locally a vicinity of the saddle-node orbit into two regions: node and saddle, see Fig. 17(left). In the node region, a trajectory is attracted to the saddle-node periodic orbit. In the saddle region, the periodic orbit is repelling. Its unstable manifold W^u consists of the trajectories which are attracted to the periodic orbit in backward time. In the forward time though, a phase point on W^u follows the bursting path: while turning around $M_{\rm lc}$ it drifts slowly rightwards, then drops onto the hyperpolarized branch of $M_{\rm eq}$, along which it slides leftward towards the fold, from there it takes off landing back on $M_{\rm lc}$. It is *imperative* for the blue-sky catastrophe that the phase point lands onto $M_{\rm lc}$ on the left from the saddle-node periodic orbit. This can be always achieved by moving the hump to the proper position relative the lower fold on $M_{\rm eq}$. Thus, the unstable manifold W^u becomes homoclinic to the saddle-node periodic orbit; this is the second component of the blue-sky catastrophe.

Therefore, at the bifurcation for some α_0 the system possesses the saddle-node periodic orbit $L_{\rm sn}$ whose two-dimensional unstable manifold W^u returns to the periodic orbit making infinitely many rotations in the node (attracting) region on the left from the strongly stable manifold W^{ss}. As

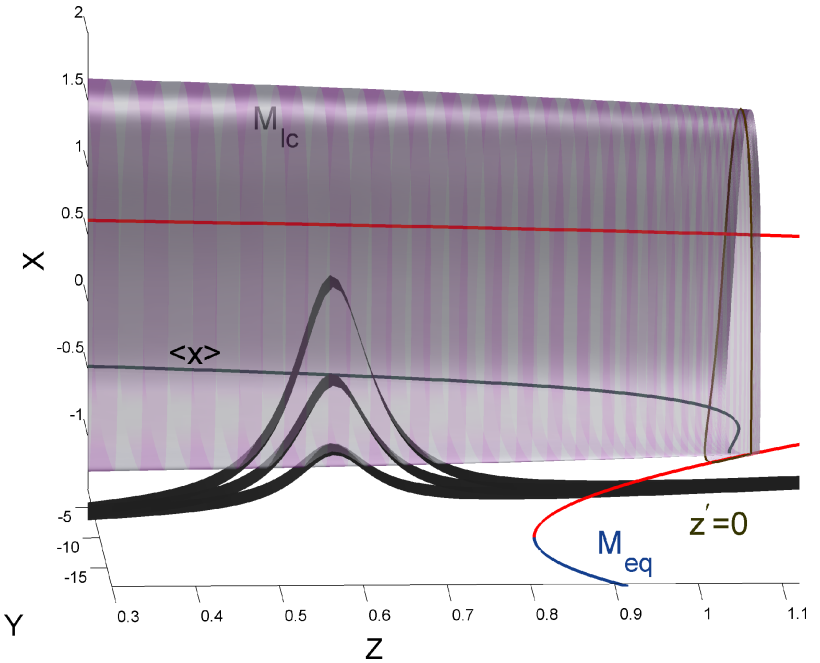

Fig. 16. Elevating the hump of the slow nullcline gives rise to the new intersection points of the slow nullcline with the average branch $\langle x \rangle$, and as a result, to the emergence of stable and saddle periodic orbits on the spiking manifold $M_{\rm lc}$.

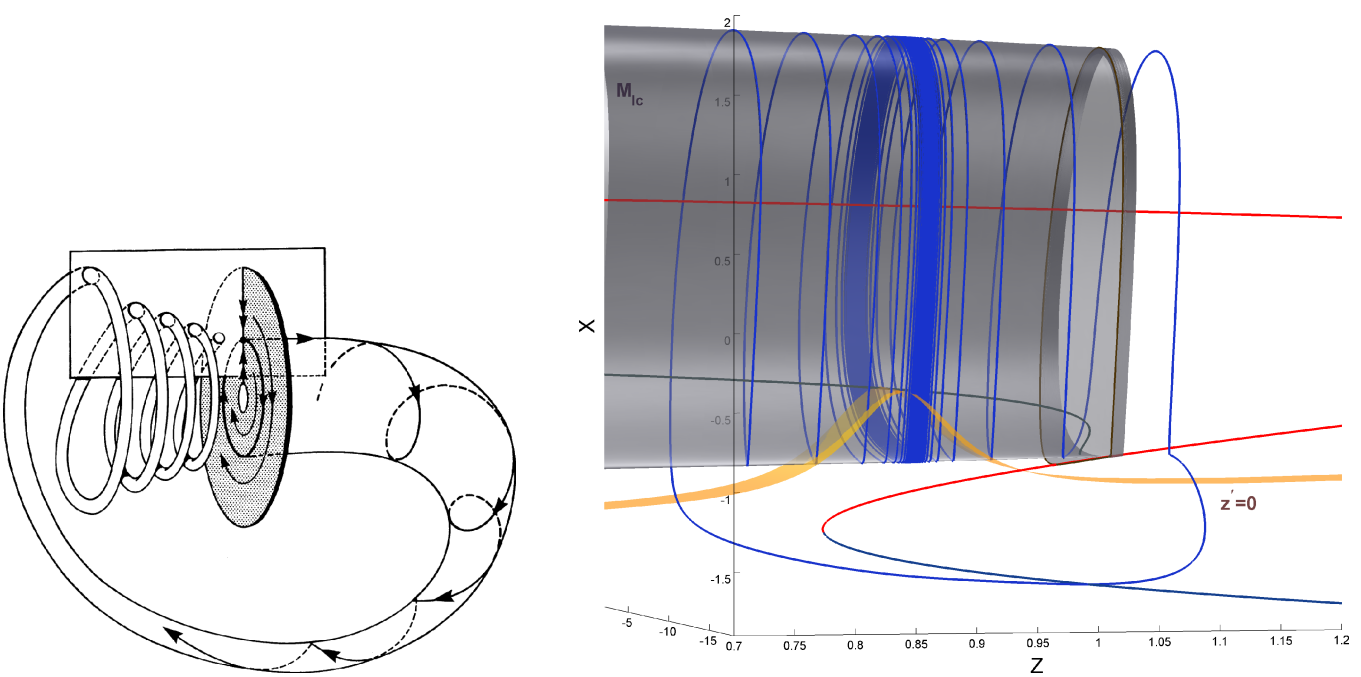

Fig. 17. (Left) Configuration of the blue-sky catastrophe proposed by Shilnikov and Turaev, from [Shilnikov *et al.*, 2001]. (Right) Blue-sky catastrophe in the HR model at $\varepsilon = 0.002$, $x_0 = -1.4$, $\alpha = 0.0083$, $z_0 = 0.9$. While passing by the phantom of the saddle-node periodic orbit, the bursting one gains more spikes thus raising its period. The interburst interval remains nearly the same.

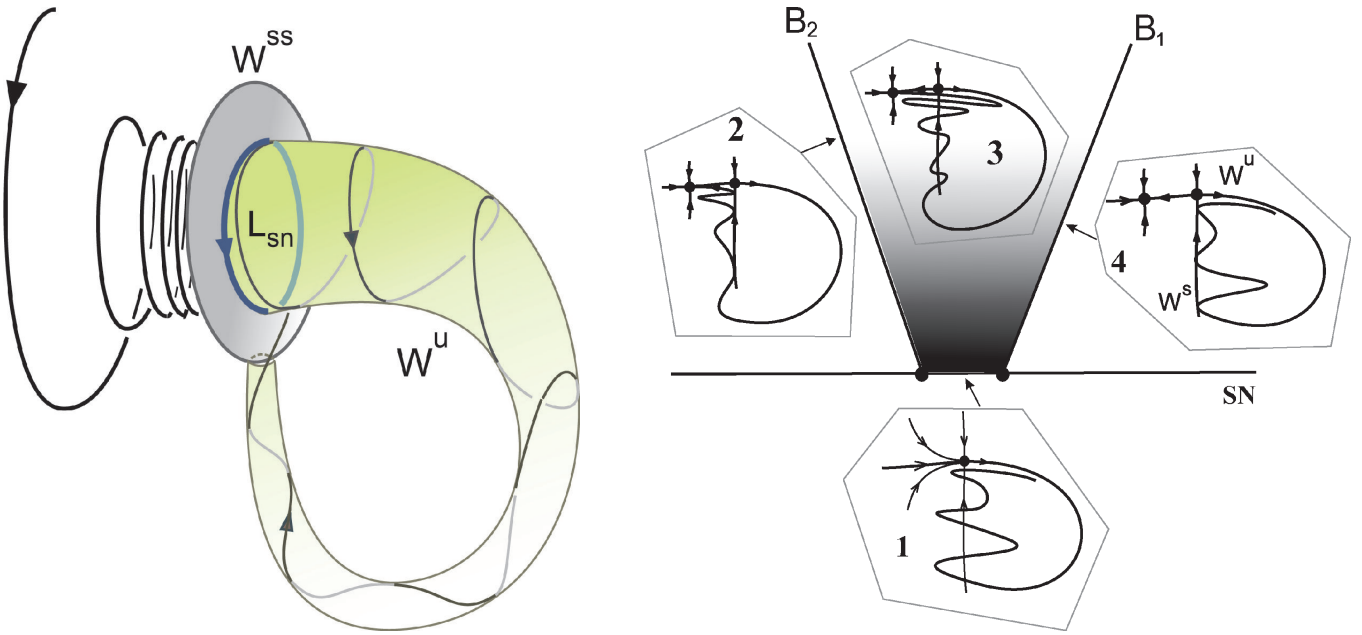

Fig. 18. (Left) Saddle-node periodic orbit $L_{\rm sn}$ with noncentral homoclinic orbits: its unstable manifold W^u returns to the orbit crossing transversally its nonleading or strongly stable manifold W^{ss}. The latter separates the node region (on the left from W^{ss}) where the bifurcating periodic orbit is stable, from the saddle region. (Right) Partial unfolding of the Lukyanov–Shilnikov bifurcation. Here, the stable and saddle fixed points correspond to the periodic orbits of the same types. The two bifurcation curves, B_1 and B_2 correspond to the primary and final homoclinic tangencies between the stable and unstable manifolds of the saddle orbit. In simple terms: to the right of B_1 the system shows the bi-stability, while on the left from B_2 the tonic spiking attractor dominates over the dynamics. In between, the dynamics is of finite-shift type, i.e. the system generates a chaotic bursting behavior terminating, sooner or later, in the regular tonic spiking. The complex dynamics persists also after the disappearance of the saddle-node point beneath the segment indicated on the bifurcation curve SN. The size of the segment is that of the unstable manifold W^u when it reaches the saddle-node orbit. From [Shilnikov *et al.*, 2005].

we lower the hump for $\alpha < \alpha_0$, the tangency is gone, and the saddle-node periodic orbit disappears. Endowed with the property of a strong contraction in the transverse direction along the hyperpolarized branch of $M_{\rm eq}$, which is composed of the stable equilibria of the slow subsystem of the HR model, the blue-sky bifurcation results in the appearance of a new stable periodic orbit of infinite period and length. The infinite period of the periodic bursting is due to the slow passage of the phase point through the "phantom" of the disappeared saddle-node orbit. This corresponds to long bursting in the model. The further the system is away from the bifurcation, the shorter is the bursting orbit. So, by approaching or leaving the bifurcation value, we can control very effectively the burst duration only, which is evaluated as $1/\sqrt{\alpha - \alpha_0}$, which is the law obeyed by a saddle-node bifurcation. Controlling burst durations has turned out to be a crucial skill for a rhythmogenesis of central pattern generators [Belykh & Shilnikov, 2008] and [Shilnikov *et al.*, 2008]. Note that the interburst interval is not affected by these manipulations. Thus, a continuous transition between the bursting into tonic spiking is achieved by changes of a single parameter of the system.

7.3. *Lukyanov–Shilnikov bifurcation and bi-stability*

The blue-sky catastrophe takes place on a codimension-one surface in the parameter space of the slow-fast system. The boundary of this surface corresponds to a jump of the phase point from the low fold of the hyperpolarized branch of the manifold $M_{\rm eq}$ right onto the strongly stable manifold W^{ss} of the saddle-node periodic orbit on the surface $M_{\rm lc}$ of fast oscillations. Such configuration leads to the onset of the Lukyanov–Shilnikov bifurcation [Lukyanov & Shilnikov, 1978] in a slow-fast system. This results in the emergence of Poincaré homoclinic orbits that cause complex shift dynamics in the system. In the singularly-perturbed systems, the magnitude of the homoclinic tangles is

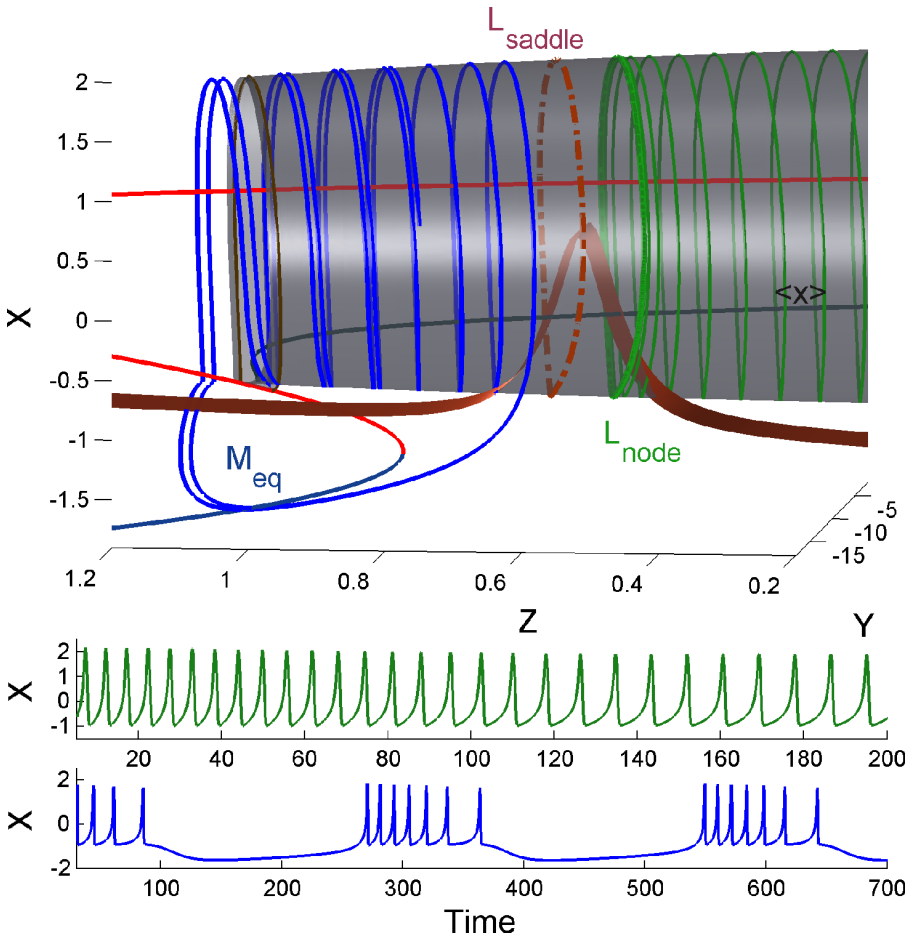

Fig. 19. Co-existence of tonic spiking and bursting in the HR model. This type of behavior takes place to the left of the bifurcation curve B_2 (inset 2) in Fig. 18.

about $\sim e^{-1/\varepsilon}$, which makes the chaotic dynamics very difficult to detect. However, the other, more evident feature of this bifurcation is bi-stability, where a spiking stable periodic orbit co-exists with a large bursting one [Cymbalyuk & Shilnikov, 2005; Shilnikov *et al.*, 2005; Cymbalyuk *et al.*, 2005]. This bi-stability is illustrated in Fig. 19 for the HR model. The bi-stability is seized as soon as the bursting trajectory becomes a homoclinic one to the separating saddle periodic orbit (Fig. 20). Moreover, the period of the bursts increases logarithmically fast as $|\ln(\alpha - \alpha_0)|$, like at all cod-1 homoclinic bifurcations of saddle orbits. This observation should help one differentiate between various transitions between tonic spiking and bursting in neuron models.

The Lukyanov–Shilnikov bifurcation describes a merge of a stable periodic orbit, representing tonic spiking oscillations in the system, with a saddle periodic orbit having transverse homoclinic trajectories, which represent bursting in the limit. This implies that at critical parameter values the system will exhibit chaotic intermittency, i.e. generate an arbitrarily long train of bursts with an unpredictably changing number of spikes within each one, prior to ultimately settling down into the periodic spiking. This intermittency is also a consequence of Smale horseshoe dynamics [Gavrilov & Shilnikov, 1973].

Since a typical intersection of two 2D surfaces in $\mathbb{R}^3$ is transverse, the presence of the noncentral homoclinic connections to the saddle-node orbit does not raise the codimension of this bifurcation. The unfolding of the bifurcation is sketched in Fig. 18(right). This bifurcation is described best by using a two-dimensional Poincaré mapping defined in some cross-section transverse to the periodic orbits. The point where a periodic orbit hits the cross-section is a fixed point of the Poincaré map. The stability of the fixed points and the stability of

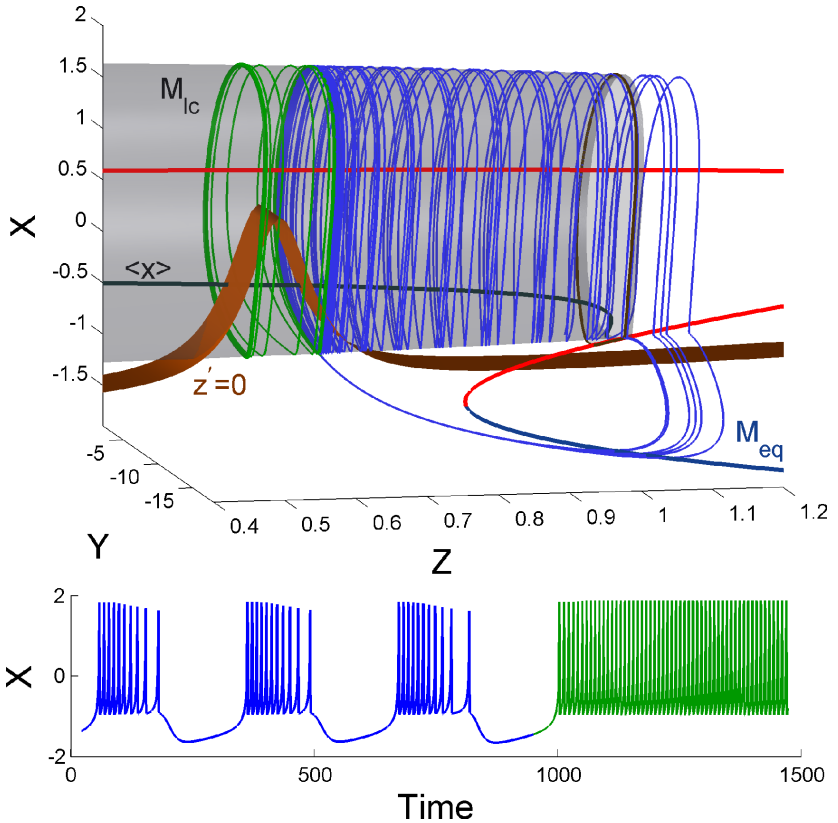

Fig. 20. Transient bursting into tonic spiking: a number of bursts are generated before the model goes into tonic spiking at $\alpha = 0.02$ and $z_0 = 0.5814335$. This corresponds to inset 3 in Fig. 18.

the periodic orbits match. In the case of the saddle-node periodic orbit, there is a single fixed point with a multiplier equal +1; this occurs on the bifurcation curve SN in Fig. 18.

Because the saddle-node fixed point has non-central homoclinic orbits generated by transverse crossings of its unstable and strongly stable manifolds, it follows that after the fixed points decouple, the saddle one will inherit the transverse homoclinic structure; this implies that the system must possess a complex shift-dynamics for the parameter values above SN within the wedge. Its boundaries correspond to the very first and last contacts between the stable and unstable manifolds of the saddle fixed point. This dynamics in this region is associated with the existence of Smale horseshoes due to transverse intersections of the stable and unstable manifolds of the saddle point. As both points disappear through the saddle-node bifurcation, the hyperbolic subset nevertheless persists, so that the complex dynamics is still observed in the parameter region beneath the indicated sector. It is the main feature of the given homoclinic saddle-node bifurcation.

The bi-stability in the HR model is shown in Fig. 19. Depending on an initial condition, the system may generate tonic spiking, if the initial point is in the attraction domain of the stable periodic orbit, or it generates bursting activity otherwise. The saddle periodic orbit separates the attraction domains of both regimes.

When the parameter α is increased, the stable and unstable periodic orbits move farther apart, so that the unstable manifold of the saddle orbit may no longer bound the attraction basin of the stable orbit. Here, the model is able to produce arbitrarily long trains of chaotic bursts before switching into periodic spiking, as shown in Fig. 20. Observe that the duration of bursting phase may grow with no upper bound as the control parameter is moved toward the transition value between the regimes as the phase point stays closer to the saddle periodic orbit; as before, this does not affect the interburst interval.

This intermittency in the model occurs "between" the corresponding boundaries B_1 and B_2 in Fig. 18. This is another consequence of the complex shift dynamics due to homoclinic wiggles

pictured there as well. The width of the parameter interval corresponding to the intermittency is small in a singularly perturbed system. Furthermore, it is proportional to the diameter of the tube of the unstable manifold W^u, which is shrinking while it returns to the saddle-node periodic orbit. Recall that the low hyperpolarized branch of M_{eq} is comprised of the stable equilibria of the fast subsystem of the HR model. In virtue of Liouville's theorem, an estimate for volume compression is given by $e^{-\lambda\tau}$ where τ is the interburst interval, and $-\lambda$ is the largest Lyapunov exponent of the stable equilibria forming this branch of M_{eq}. This makes the intermittency hard but rewarding to find in a slow fast system.

Acknowledgments

We are grateful to Rene Gordon for comments and suggestions. A. L. Shilnikov's research is supported by the GSU Brains & Behavior Program and RFFI Grant No. 050100558.

References

Abraham, R. H. [1985] "Chaostrophes, intermittency, and noise," in *Chaos*, *Fractals*, *and Dynamics*, Conf. Univ. Guelph/Can. 1981 and 1983, Lecture Notes Pure Appl. Math. **98**, pp. 3–22.

Andronov, A. A. & Leontovich, E. A. [1937] "Some cases of dependence of limit cycles on a parameter," *Uchenye zapiski Gorkovskogo Universiteta* **6**, 3–24.

Andronov, A. A., Vitt, A. A. & Khaikin, S. E. [1966] *Theory of Oscillations*, International Series of Monographs in Physics, Vol. 4 (Pergamon Press, Oxford).

Andronov, A. A., Leontovich, E. A., Gordon, I. E. & Maier, A. G. [1971] *The Theory of Bifurcations of Dynamical Systems on a Plane*, Israel Program of Scientific Translation, Jerusalem.

Arnold, V. I., Afrajmovich, V. S., Ilyashenko, Yu. S. & Shil'nikov, L. P. [1984] *Bifurcation Theory*, *Dynamical Systems V*, Encyclopaedia of Mathematical Sciences (Springer-Verlag).

Bazhenov, M., Timofeev, I., Steriade, M. & Sejnowski, T. J. [2000] "Spiking-bursting activity in the thalamic reticular nucleus initiates sequences of spindle oscillations in thalamic networks," *J. Neurophysiol.* **84**, 1076–1087.

Belykh, V. N., Belykh, I. V., Colding-Joregensen, M. & Mosekilde, E. [2000] "Homoclinic bifurcations leading to bursting oscillations in cell models," *Eur. Phys. J. E* **3**, 205–214.

Belykh, V., Belykh, I. & Mosekilde, E. [2005a] "The hyperbolic Plykin attractor can exist in neuron models," *Int. J. Bifurcation and Chaos* **15**, 1112–1130.

Belykh, I., de Lange, E. & Hasler, M. [2005b] "Synchronization of bursting neurons: what matters in the network topology," *Phys. Rev. Lett.* **94**, 188101–188105.

Belykh, I. V. & Shilnikov, A. [2008] "When weak inhibition synchronizes strongly desynchronizing network of bursting neurons," *Phys. Rev. Lett.*, in press.

Benoit, E., Callot, J.-L., Diener, F. & Diener, M. [1981] "Chasse au canard," *Collect. Math.* **32**, 37–119.

Bertram, R. [1993] "A computational study of the effects of serotonin on a molluscan burster neuron," *Biol. Cybern.* **69**, 257–267.

Bertram, R., Butte, M. J., Kiemel, T. & Sherman, A. [1995] "Topological and phenomenological classification of bursting oscillations," *Bull. Math. Biol.* **57**, 413–439.

Bertram, R. & Sherman, A. [2000] "Dynamical complexity and temporal plasticity in pancreatic beta-cells," *J. Biosci.* **25**, 197–209.

Best, J., Borisyuk, A, Rubin, J., Terman, D. & Wechselberger, M. [2005] "The dynamic range of bursting in a model respirator pacemaker network," *SIAM J. Appl. Dyn. Syst.* **4**, 1107–1139.

Butera, R. [1998] "Multirhythmic bursting," *Chaos* **8**, 274–282.

Callot, J.-L., Diener, F. & Diener, M. [1978] "Le probléme de la chasse au canard," *C. R. Acad. Sci.* **286**, 1059.

Canavier, C. C., Baxter, D. A., Clark, L. & Byrne, J. [1993] "Nonlinear dynamics in a model neuron provide a novel mechanism for transient synaptic inputs to produce long-term alterations of postsynaptic activity," *J. Neurophysiol.* **69**, 2252–2270.

Channell, P., Cymbalyuk, G. & Shilnikov, A. L. [2007a] "Applications of the Poincare mapping technique to analysis of neuronal dynamics," *Neurocomputing* **70**, 10–12.

Channell, P., Cymbalyuk, G. & Shilnikov, A. L. [2007b] "Origin of bursting through homoclinic spike adding in a neuron model," *Phys. Rev. Lett.* **98**, 134101–134105.

Chay, T. R. & Keizer, J. [1983] "Minimal model for membrane oscillations in the pancreatic beta-cell," *Biophys. J.* **42**, 181–190.

Chay, T. R. [1985] "Chaos in a three-variable model of an excitable cell," *Physica D* **16**, 233–242.

Chow, S.-B., Deng, B. & Fiedler, B. [1990] "Homoclinic bifurcations of resonant eigenvalues," *J. Dyn. Diff. Eqs.* **2**, 177–245.

Coombses, S. & Bressloff, P. (eds.) [2005] *Bursting*: *The Genesis of Rhythm in the Neurvous System* (World Scientific, Singapore).

Cymbalyuk, G. S. & Calabrese, R. L. [2001] "A model of slow plateau-like oscillations based upon the fast Na+ current in a window mode," *Neurocomputing* **38–40**, 159–166.

Cymbalyuk, G., Gaudry, Q., Masino, M. A. & Calabrese, R. L. [2002] "A model of a segmental oscillator in the leech heartbeat neuronal network," *J. Neurosci.* **22**, 10580–10587.

Cymbalyuk, G. & Shilnikov, A. L. [2005] "Co-existent tonic spiking modes in a leech neuron model," *J. Comput. Neurosci.* **18**, 255–263.

Deng, B. [1993] "Homoclinic twisting bifurcation and cusp horseshoe maps," *J. Dyn. Diff. Eqs.* **5**, 417–467.

Deng, B. & Hines, G. [2002] "Food chain chaos due to Shilnikov's orbit," *Chaos* **12**, 533–538.

Deng, B. [2004] "Food chain chaos with canard explosion," *Chaos* **14**.

Doiron, B., Laing, C. & Longtin, A. [2002] "Ghostbursting: A novel neuronal burst mechanism," *Comp. Neurosci.* **12**, 5–15.

Dumortier, F. & Roussarie, R. [1996] "Canard cycles and center manifolds," *Mem. Amer. Math. Soc.* **121**, 101–121.

Ermentrout, B. & Kopell, N. [1991] "Multiple pulse interactions and averaging in systems of coupled neural oscillators," *J. Math. Biol.* **29**, 195–217.

Fenichel, N. [1979] "Geometric singular perturbation theory for ordinary differential equations," *J. Diff. Eqs.* **31**, 53–98.

Feudel, U., Neiman, A., Pei, X., Wojtenek, W., Braun, H., Huber, M. & Moss, F. [2000] "Homoclinic bifurcation in a Hodgkin–Huxley model of thermally sensitive neurons," *Chaos* **10**, 231–239.

Frohlich, F. & Bazhenov, M. [2006] "Coexistence of tonic firing and bursting in cortical neurons," *Phys. Rev. E* **74**, 031922–031929.

Gavrilov, N. K. & Shilnikov, L. P. [1973] "On three-dimensional dynamical systems close to systems with a structurally unstable homoclinic curve," *Math. USSR-Sb.* **19**, 139–150.

Gavrilov, N. K. & Shilnikov, A. L. [2000] "Example of a blue sky catastrophe," in *Methods of Qualitative Theory of Differential Equations and Related Topics*, AMS Transl. Series II, **200**, pp. 99–105.

Gradstein, I. S. [1946] "On behaviour of solutions of systems of linear differential equations degenerating in the limit," *Dokl. Acad. Sci. URSS* **53**, 391–394.

Gu, H., Yang, M., Li, L., Liu, Z. & Ren, W. [2003] "Dynamics of autonomous stochastic resonance in neural period adding bifurcation scenarios," *Phys. Lett. A* **319**, 89–96.

Guckenheimer, J., Gueron, S. & Harris-Warrick, R. M. [1993] "Mapping the dynamics of a bursting neuron," *Philos. Trans. Royal Soc. Lond. Biol. Sci.* **341**, 345–359.

Guckenheimer, J. [1996] "Towards a global theory of singularly perturbed systems," in *Progr. Nonlin. Diff. Eqs. Their Appl.* **19**, 214–225.

Guckenheimer, J. & Willms, A. [2000] "Analysis of a subcritical Hopf-homoclinic bifurcation," *Physica D* **139**, 195–216.

Hill, A., Lu, J., Masino, M., Olsen, O. & Calabrese, R. L. [2001] "A model of a segmental oscillator in the leech heartbeat neuronal network," *J. Comput. Neurosci.* **10**, 281–302.

Hindmarsh, J. L. & Rose, R. M. [1984] "A model of neuronal bursting using three coupled first-order differential equations," *Proc. Roy. Soc. Lond. B* **221**, 87.

Hodgkin, A. L. & Huxley, A. F. [1952] "A quantitative description of membrane current and its application to conduction and excitation in nerve," *J. Physiol.* **117**, 500–544.

Holden, A. V. & Fan, Y. S. [1992] "From simple to simple bursting oscillatory behaviour via intermittent chaos in the Rose–Hindmarsh model for neuronal activity," *Chaos Solit. Fract.* **2**, 221–230.

Huerta, R., Rabinovich, M., Abarbanel, H. & Bazhenov, M. [1997] "Spike-train bifurcation scaling in two coupled chaotic neurons," *Phys. Rev. E* **55**, 2108–2110.

Izhikevich, E. M. [2000] "Neural excitability, spiking and bursting," *Int. J. Bifurcation and Chaos* **10**, 1171–1266.

Izhikevich, E. M. [2004] "Which model to use for cortical spiking neurons?" *IEEE Trans. Neural Networks* **12**, 1063–1107.

Jones, C. K. R. T. & Kopell, N. [1994] "Tracking invariant manifolds with differential forms in singularly perturbed systems," *J. Diff. Eqs.* **108**, 64–88.

Kopell, N. [1998] "Toward a theory of modelling central pattern generators," in *Neural Control of Rhythmic Movements in Vertebrates*, eds. Cohen, A. H., Rossignol, S. & Grillner, S. (Wiley, NY), pp. 23–33.

Kramer, M. A., Traub, R. D. & Kopell, N. [2008] *New Dynamics in Cerebeller Purkinje Cells: Torus Canards.*

Krupa, M. & Szmolyan, P. [2001] "Extending geometric singular perturbation theory to nonhyperbolic points — fold and canard points in two dimensions," *SIAM J. Math. Anal.* **33**, 286–314.

Kuznetsov, Yu. A. & Rinaldi, S. [1996] "Remarks on food chain dynamics," *Math. Biosciences* **134**, 1–33.

Kuznetsov, Yu. A. [1998] *Elements of Applied Bifurcation Theory*, 2nd updated ed., Applied Mathematical Sciences, Vol. 112 (Springer, NY). CONTENTS is available at ftp://ftp.cwi.nl/pub/CONTENT.

Laing, C. R., Doiron, B., Longtin, A., Noonan, L., Turner, R. W. & Maler, L. [2003] "Type I burst excitability," *J. Comput. Neurosci.* **14**, 329–335.

Leontovich, E. A. [1951] "On birth of limit cycles from separatrices," *DAN SSSR* **74**, 641–644.

Lukyanov, V. & Shilnikov, L. P. [1978] "On some bifurcations of dynamical systems with homoclinic structures," *Sov. Math. Dokl.* **19**, 1314–1318.

Malaschenko, T., Shilnikov, A. L. & Cymbalyuk, G. [2008] "Subtheshold oscillations in a neuron model," *J. Comp. Neurosci.*, to be submitted.

Medvedev, G. M. [2006] "Transition to bursting via deterministic chaos," *Phys. Rev. Lett.* **97**, 048102.

Mischenko, E. F. & Rozov, N. Kh. [1980] *Differential Equations with Small Parameters and Relaxation Oscillations* (Plenum Press).

Mischenko, E. F., Kolesov, Yu. S., Kolesov, A. Yu. & Rozov, N. Kh. [1984] *Asymptotic Methods in Singularly Perturbed Systems*, Monographs in Contemporary Mathematics (Consultants Bureau, NY).

Nozdracheva, V. P. [1982] "Bifurcation of a noncoarse separatrix loop," *Diff. Eqs.* **18**, 1098–1104.

Pontryagin, L. S. & Rodygin, L. V. [1960] "Periodic solution of a system of ordinary differential equations with a small parameter in the terms containing derivatives," *Sov. Math. Dokl.* **1**, 611–661.

Rinzel, J. [1985] "Bursting oscillations in an excitable membrane model," in *Ordinary and Partial Differential Equations*, Lecture Notes in Mathematics, Vol. 1151, pp. 304–320.

Rinzel, J. & Ermentrout, B. [1989] "Analysis of neural excitability and oscillations," in *Methods of Neural Modeling*: *From Synapses to Networks*, eds. Koch, C. & Segev, I. (MIT Press), pp. 135–169.

Robinson, C. [1989] "Homoclinic bifurcation to a transitive attractor of Lorenz type," *Nonlinearity* **2**, 495–518.

Rosenblum, M. G. & Pikovsky, A. S. [2004] "Controlling synchronization in an ensemble of globally coupled oscillators," *Phys. Rev. Lett.* **92**, 114102–114106.

Rowat, P. F. & Elson, R. C. [2004] "State-dependent effects of Na channel noise on neuronal burst generation," *J. Comput. Neurosci.* **16**, 87–112.

Rychlik, M. [1990] "Lorenz attractor through Shilnikov type bifurcation," *Erg. Th. Dyn. Syst.* **10**, 793–821.

Shilnikov, A. L. [1986] "Bifurcations and chaos in the Shimizu–Marioka system," [In Russian], in *Methods and Qualitative Theory of Differential Equations*, *Gorky State University*, pp. 180–193; [1991] English translation in Selecta Mathematica Sovietica **10**, 105–117.

Shilnikov, A. L. [1993] "On bifurcations of the Lorenz attractor in the Shimizu–Marioka system," *Physica D* **62**, 338–346.

Shilnikov, A. L., Shilnikov, L. P. & Turaev, D. V. [1993] "Normal forms and Lorenz attractors," *Int. J. Bifurcation and Chaos* **3**, 1123–1139.

Shilnikov, A. L. & Rulkov, N. F. [2003] "Origin of chaos in a two-dimensional map modelling spiking-bursting neural activity," *Int. J. Bifurcation and Chaos* **13**, 3325–3340.

Shilnikov, A. L. & Cymbaluyk, G. [2004] "Homoclinic saddle-node orbit bifurcations en route between tonic spiking and bursting in neuron models. Invited paper," *Regular & Chaotic Dyn.* **9**, 1–34.

Shilnikov, A. L. & Rulkov, N. F. [2004] "Subthreshold oscillations in a map-based neuron model," *Phys. Lett. A* **328**, 177–184.

Shilnikov, A. L., Shilnikov, L. P. & Turaev, D. V. [2004] "Mathematical aspects of classical synchronization theory, Tutorial," *Int. J. Bifurcation and Chaos* **14**, 2143–2160.

Shilnikov, A. L., Calabrese, R. L. & Cymbaluyk, G. [2005a] "How a neuron model can demonstrate coexistence of tonic spiking and bursting?" *Neurocomputing* **65–66**, 869–875.

Shilnikov, A. L., Calabrese, R. L. & Cymbalyuk, G. [2005b] "Mechanism of bi-stability: tonic spiking and bursting in a neuron model," *Phys. Rev. E* **71**, 205–214.

Shilnikov, A. L. & Cymbalyuk. G. [2005] "Transition between tonic-spiking and bursting in a neuron model via the blue-sky catastrophe," *Phys. Rev. Lett.* **94**, 048101–048105.

Shilnikov, A. L., Shilnikov, L. P. & Turaev, D. V. [2005c] "Blue sky catastrophe in singularly perturbed systems," *Moscow Math. J.* **5**, 205–218.

Shilnikov, A. L. & Kolomiets, M. L. [2008] "Bursting manifolds of neuronal models," *Int. J. Bifurcation and Chaos*, to be submitted.

Shilnikov, A. L., Gordon, R. & Belykh, I. V. [2008] "Polyrhytmic synchronization in bursting network motifs," *J. Chaos* **18**, in press.

Shilnikov, A. L. & Turaev, D. V. [2008] "Singular orbit-flip bifurcation in slow-fast systems," in preparation.

Shilnikov, L. P. [1965] "Case of the existence of a denumerable set of periodic motions," *Sov. Math. Dokl.* **6**, 163–166.

Shilnikov, L. P. & Turaev, D. V. [1997] "On simple bifurcations leading to hyperbolic attractors," *Comput. Math. Appl.* **34**, 441–457.

Shilnikov, L. P., Shilnikov, A. L., Turaev, D. V. & Chua, L. [1998] *Methods of Qualitative Theory in Nonlinear Dynamics. Part I* (World Scientific, Singapore).

Shilnikov, L. P. & Turaev, D. V. [2000] "A new simple bifurcation of a periodic orbit of blue sky catastrophe type," in *Methods of Qualitative Theory of Differential Equations and Related Topics*, AMS Transl. Series II, **200**, pp. 165–188.

Shilnikov, L. P., Shilnikov, A. L., Turaev, D. V. & Chua, L. [2001] *Methods of Qualitative Theory in Nonlinear Dynamics. Part II* (World Scientific, Singapore).

Terman, D. [1992] "The transition from bursting to continuous spiking in an excitable membrane model," *J. Nonlin. Sci.* **2**, 133–182.

Tikhonov, A. N. [1948] "On the dependence of solutions of differential equations from a small parameter," *Mat. Sb.* **2**, 193–204.

Turaev, D. V. & Shilnikov, L. P. [1995] "Blue sky catastrophes," *Dokl. Math.* **51**, 404–407.

Wang, X. J. [1993] "Genesis of bursting oscillations in the Hindmarsh–Rose model and homoclinicity to a chaotic saddle," *Physica* **62**, 263–274.

Wang, X. J. & Rinzel, J. [1995] "Oscillatory and bursting properties of neurons," in *The Handbook of Brain Theory and Neural Networks*, ed. Arbib, M. (MIT Press), pp. 686–691.

Yang, Z., Lu, Q. & Li, L. [2006] "The genesis of period-adding bursting without bursting-chaos in the Chay model chaos," *Solit. Fract.* **27**, 689–697.